Manuscript Details

Manuscript number	QUAGEO_2019_55
Title	LUMINESCENCE DATING OF QUARTZ AND FELDSPARS AT MWULU'S CAVE (LIMPOPO, SOUTH AFRICA)
Article type	Research paper

Abstract

Luminescence dating is applied to sediments from Mwulu's Cave, whose lithics are typologically Middle Stone Age (MSA) and have been previously assigned to what is called the Pietersburg industry. This industry is, however, poorly defined both chronologically and typologically. Luminescence methods were applied to both quartz and potassium feldspars by two different laboratories. Age results from single-grain quartz are much younger than those from multi-grain aliquots and this is attributed to the high number of saturated grains that are removed in the single-grain analysis but whose signals are often retained in the multi-grain analysis. Single-grain potassium feldspar ages are much older than the single-grain quartz ages. Application of various methods to address anomalous fading produced broadly consistent results among samples. Although precise ages are hard to pin point, partly because of post-depositional mixing, potassium feldspar ages for the sequence appear to converge about 60-70 ka, or slightly older for the stratigraphically lowest sample. These are compared to other South African MSA sequences and industries.

Keywords	Luminescence; Quartz; Potassium feldspar; Huntley-Lamothe method; IRSL; Middle Stone Age

Corresponding Author	Paloma de la Pena
Corresponding Author's Institution	Evolutionary Studies Institute
Order of Authors	James Feathers, M Evans, Dominic Stratford, Paloma de la Pena

Suggested reviewers	Lamothe Michel, Georgina King

Submission Files Included in this PDF

File Name [File Type]

Cover Letter.docx [Cover Letter]

Mwulus Final_FINAL.docx [Manuscript File]

Fig1.tif [Figure]

Fig2 .tif [Figure]

Fig3.tif [Figure]

Fig4.tif [Figure]

S1.tif [Figure]

S2.tif [Figure]

S3.tif [Figure]

S4.tif [Figure]

S5.tif [Figure]

S6.tif [Figure]

S7.tif [Figure]

S8.tif [Figure]

S9.tif [Figure]

S10.tif [Figure]

S11.tif [Figure]

Table 1.docx [Figure]

Table 2.docx [Figure]

Table 3.docx [Figure]

Table 4.docx [Figure]

Table 5.docx [Figure]

Table 6.docx [Figure]

Table 7.docx [Figure]

Table 8.docx [Figure]

Table 9.docx [Figure]

No conflict of interest.docx [Conflict of Interest]

To view all the submission files, including those not included in the PDF, click on the manuscript title on your EVISE Homepage, then click 'Download zip file'.

Research Data Related to this Submission

There are no linked research data sets for this submission. The following reason is given:
Data will be made available on request

Dear Editor,

Please consider our paper:

LUMINESCENCE DATING OF QUARTZ AND FELDSPARS AT MWULU'S CAVE

(LIMPOPO, SOUTH AFRICA)

The material in the paper is entirely new and is not being considered for publication elsewhere. We declare no conflict of interest and agree to the submission of the paper. This paper is a research article and is worthy of consideration for publication in *Quaternary Geochronology* because:

Luminescence dating is applied to sediments from Mwulu's Cave, whose lithics are typologically Middle Stone Age (MSA) and have been previously assigned to what is called the Pietersburg industry. This industry is, however, poorly defined both chronologically and typologically. Luminescence methods were applied to both quartz and potassium feldspars by two different laboratories. Age results from single-grain quartz are much younger than those from multi-grain aliquots and this is attributed to the high number of saturated grains that are removed in the single-grain analysis but whose signals are often retained in the multi-grain analysis. Single-grain potassium feldspar ages are much older than the single-grain quartz ages. Application of various methods to address anomalous fading produced broadly consistent results among samples. Although precise ages are hard to pin point, partly because of post-depositional mixing, potassium feldspar ages for the sequence appear to converge about 60-70 ka, or slightly older for the stratigraphically lowest sample. These are compared to other South African MSA sequences and industries.

Corresponding author:

Paloma de la Peña

paloma.delapenya@gmail.com

Researcher

Evolutionary Studies Institute, University of Witwatersrand, Yale Road, Johannesburg, South Africa.

The rest of the authors:

James K. Feathers

Luminescence Dating Laboratory, University of Washington, Seattle, WA 98195-3412

Mary Evans

School of Geography, Archaeology and Environmental studies. University of the Witwatersrand. South Africa

Dominic J. Stratford

School of Geography, Archaeology and Environmental studies. University of the Witwatersrand. South Africa

The recommended reviewers are:

Georgina King (georgina.king@unil.ch) or Michel Lamothe (lamothe.michel@uqam.ca).

Thank you for your attention,

Yours sincerely,

Paloma de la Peña

Johannesburg, 8th July 2019

LUMINESCENCE DATING OF QUARTZ AND FELDSPARS AT MWULU'S CAVE (LIMPOPO, SOUTH AFRICA)

Feathers, J. K.[1], Evans, M.[2], Stratford, D. J.[2], and de la Peña, P[3,*].

1. Luminescence Dating Laboratory, University of Washington, Seattle, WA 98195-3412

2. School of Geography, Archaeology and Environmental studies. University of the Witwatersrand. South Africa

3. Evolutionary Studies Institute. University of the Witwatersrand. South Africa

*Corresponding author: paloma.delapenya@gmail.com

Keywords

Luminescence, *Quartz*, *Potassium feldspar*, Huntley-Lamothe method, IRSL , *Middle Stone Age*

Abstract

Luminescence dating is applied to sediments from Mwulu's Cave, whose lithics are typologically Middle Stone Age (MSA) and have been previously assigned to what is called the Pietersburg industry. This industry is, however, poorly defined both chronologically and typologically. Luminescence methods were applied to both quartz and potassium feldspars by two different laboratories. Age results from single-grain quartz are much younger than those from multi-grain aliquots and this is attributed to the high number of saturated grains that are removed in the single-grain analysis but whose signals are often retained in the multi-grain analysis. Single-grain potassium feldspar ages are much older than the single-grain quartz ages. Application of various methods to address anomalous fading produced broadly consistent results among samples. Although precise ages are hard to pin point, partly because of post-depositional mixing, potassium feldspar ages for the sequence appear to converge about 60-70 ka, or slightly older for the stratigraphically lowest sample. These are compared to other South African MSA sequences and industries.

Introduction

The Southern African Middle Stone Age (300-40/20ka) chronology is currently the subject of intense scientific discussion. The Middle Stone Age (MSA) is an archaeological period first defined in Africa by Goodwin and Van Riet Lowe in 1929. In the last half century it has attracted much interest because it is associated in Sub-Saharan Africa with the first behavioral and cultural expressions of our own species *Homo sapiens* (Thackeray, 1992; Wurz, 2013; Wadley, 2015). The antiquity of the MSA only began to be understood later in the 20th century, with the development of geochronological methodologies that showed Middle Stone archaeological assemblages to be much older than the post-Pleistocene age originally proposed (Söhnge et al., 1937).

In Southern Africa the geochronological debate in the last decade have centered around the chronological status of two technological traditions within the MSA —the Howiesons Poort and the Still Bay —with different research efforts producing divergent conclusions (Jacobs et al., 2008; Tribolo et al., 2013; Feathers, 2015; Jacobs and Roberts, 2015, among others) regarding the duration, appearance and disappearance of these two technological traditions. Some suggest they were short- (5000 years or less), whereas others maintain much longer durations, as much as 50,000 for the Howiesons Poort (Tribolo et al., 2013). Scrutiny of the methodologies applied and the geological context is critical for evaluating this issue.

Mwulu's cave was excavated originally in 1947 by P.V. Tobias (1949, 1954) and subsequently revisited by P. de la Peña and colleagues in 2017 (de la Peña et al., 2018). Tobias attributed the lithics recovered from Mwulu's Cave as MSA in age and assigned them to a specific industry called the Pietersburg (Tobias, 1949, 1954). Tobias found similarities between the stone tools from Mwulu's and those from a contemporary excavations at Border Cave (Cook, Malan and Wells, 1947). Later typological analyses (Mason, 1957; Sampson, 1972, 1974; Beaumont, 1978) and archaeological synthesis (Thackeray, 1992; Wurz 2013; Wadley, 2015) maintained the label of 'Pietersburg' for Mwulu's Cave archaeological material.

Work by Peter Beaumont at Border Cave in the 1970s, first began to reveal the great antiquity of the MSA . In fact the only currently reliable ages for the so-called Pietersburg industry come from Electron Spin Resonance (ESR) applied at this time to materials from Border Cave. These dates were secured from the basal members of the stratigraphic sequence (4WA, 5BS and 5WA) and provided dates of between 100-220 ka (Grün and Beaumont 2001; Grün et al. 2003). In more recent geochronological papers the industries attributed to those layers have been labelled as 'MSA1' instead of Pietersburg (Volman 1981; Grün and Beaumont 2001; Grün et al. 2003).

The new project at Mwulu's Cave (de la Peña et al., 2018) was initiated with the following objectives: to provide a revised stratigraphy, to re-study, technologically, the archaeological material from the old excavations and the new collections, and to offer, for the first time, a chronological and palaeoenvironmental framework of the site. The ultimate goal was to include all of these data into a renewed discussion of Middle Stone Age variability spanning different biomes in the northeastern part of southern Africa.

The age range of everything that has been called "Pietersburg" is unknown, so calling a lithic industry "Pietersburg" says almost nothing about its age beyond an MSA designation. The definition of "Pietersburg" is also not clear, so typological affinities are not easily drawn either. In this paper we do

not assume “Pietersburg” is even the proper label for Mwulu’s Cave stone tools. Instead we aim to produce a chronology independent of any typological designations. Toward that end, we have applied luminescence dating from two different laboratories, which when combined with stratigraphy, begin to work out Mwulu’s chronology. As expected, the results are far from simple.

Geological Setting

Mwulu’s Cave is located on the eastern escarpment of the Makapansberg mountains near the Makapan Valley and only 5 m from Cave of Hearths (Figure 1). It is situated 30 m below an east-facing overhanging quartzite ledge, and 15 m above the base of the cliff. The cave opens five meters below a compound fracture that branches into two diverging joints. The development of the fracture is most likely responsible for the collapses that formed the cave. The 14 m deep, 4 m wide cave formed in the middle beds of the Late Archaean, Early Proterozoic quartzites of the Black Reef Formation, the basal lithostratigraphic unit of the Transvaal Supergroup (Eriksson et al. 1995; Els et al. 1995). The lithologies represented in the cliff near the Mwulu’s Cave opening range through various quartzitic facies, including medium to coarse-grained sediments with cross-bedded, upwards fining, and massive structures typical of the Black Reef Formation quartzites and sandstones (Button 1973; Henry et al. 1990; Eriksson et al. 1993, 1995). Specifically, the cave formed within an abundantly jointed coarse-grained (-1.0 – 0.5 Phi) massive quartzite, that is exposed in the walls, roof and floor. Vertical joints in the roof facilitate continual cave breakdown and penetration of water throughout the cave.

Figure 1. A. Location of Mwulu’s Cave (Limpopo, South Africa). B. Digital model of terrain with Geographical coordinates and Makapan Valley, Mwulu’s Cave and Mokopane indicated. The digital model of terrain was retrieved from https://lpdaac.usgs.gov/ maintained by the NASA EOSDIS Land Processes Distributed Active Archive Center (LP DAAC). Modified from de la Peña et al. (2018)

Natural clasts are derived from the decay of the cave and are generally low in abundance through the sedimentary sequence. At the base of the deposits near the shelter floor, however unsorted tabular natural clasts occurring in varying states of decay are more abundant. Minor additional local lithologies are represented as clasts in the deposits in the form of shales, mudstone, siltstones, sandstones, quartz crystals and iron oxide nodules in various forms. Once detached from the walls and roof, the tabular coarse-grained quartzite clasts decay in situ, rounding rapidly and contributing angular coarse sand particles to the deposits, generally larger than the grain sizes used in luminescence dating. The matrix of Mwulu’s sediments ranges from sand-sized particles (autogenic and aeolian) to a relatively minor contribution of silts. Biotic and chemical contributions to the Mwulu’s Cave sediments include abundant burnt and unburnt plant material fluctuating in quantity throughout the deposits. The consistency of poorly consolidated sandy sediments through the sequence with concentrations of moisture and organic carbon in artefact-rich levels suggests water (and by association plant growth) accumulated differentially, potentially mobilizing the finer sediment fractions.

The stratigraphy has been divided into five units (Figure 2), named I to V from the surface to the cave floor, distinguished by color, and presence of ash and organics. All three lower units have higher

organic contents than the upper units. The artifacts appear in three horizontal clusters, one in Unit I, one in Unit II and one spanning Units III-V . The clusters were defined by two grouping spatial analyses (de la Peña et al. 2018).

Figure 2. A. Tobias's stratigraphy (Tobias, 1949). B. Mwulu's Cave West profile stratigraphic sequence with total station-derived depths on the right vertical axis. The left vertical axis presents Tobias's stratigraphic divisions and nomenclature (1949, 1954) and the Units identified in the field and excavated in 2017 (I – V).

Lithics

Quartzite is the dominant raw material in all layers, and it most likely originates from the cave's host rock. Most of the cores present centripetal scar removals, suggesting a *Levallois*-like reduction. The retouched pieces are grouped into three main types: side-scrapers, notches and denticulates. Some bifacial pieces were found in the Tobias excavation, although none were found in the 2017 campaign. Triangular blanks and classic *Levallois* points are the most abundant blank shape, being particularly abundant in the three lower units. As mentioned, Mwulu's Cave has been recurrently attributed to the Pietersburg industry (Tobias 1949, 1954; Beaumont, 1978; Mason, 1957; Sampson, 1974; Porraz et al., 2018). The status of this industrial entity, after almost a century of MSA analyses is still precarious regarding the bases of its definition. An in depth analysis and comparison of the technology of the Mwulu's lithic material must be performed in the near future to clarify its status and correlations (if existing). The preliminary knowledge of the archeological technotypological characteristics have not conditioned in any sense the geochronological results here presented.

Sampling and Methods

Twelve luminescence samples were collected by driving light-tight cylinders into the profiles (Figure 3). Six were submitted to the University of Witwatersrand Geo-Luminescence Laboratory in Johannesburg and six were submitted to the Luminescence Dating Laboratory at the University of Washington in Seattle. The sampling tubes were opened in the laboratory under safe-light conditions. The sediment within 2 cm of the ends of the tubes were removed as potentially light contaminated and were used instead for dose rate determination. The inner portion of each tube was used for equivalent dose (D_e) determination. The D_e is the laboratory estimate of the total dose absorbed by the sample through time. The Witwatersrand lab processed only quartz for this, while the Washington lab processed both quartz and potassium feldspar.

Figure 3. Location of the twelve sediment samples taken for luminescence. The identified as pink were sent to Witwatersrand University, whereas the identified here as yellow were sent to University of Washington. Each section of the scale is 10cm.

The material was sieved to 180-212µm grain size, treated with HCl and H_2O_2 to remove carbonates and organics and then placed in a heavy liquid medium to isolate quartz (<2.67 specific gravity) and potassium feldspar (<2.58). The quartz was etched for 40 minutes with 40 or 48% HF to degrade any remaining feldspar and to remove the alpha effected outer layer of the grains. The etch

was followed by a HCl wash to remove any acid soluble fluorides. No HF treatment was given to the feldspar fraction.

D_e was determined on multi-grain 1-mm diameter single-aliquots at the Witwatersrand lab and on single-grains at the Washington lab. The Witwatersrand lab used 470 nm diodes (40mW/cm^2) constrained by a green long pass (GG-420) filter to stimulate quartz grains on a Risø TL/OSL-DA-15 reader. The Washington lab used a 540nm green laser (45 W/cm^2) to stimulate quartz grains also on a Risø TL/OSL-DA-15 reader and a 150mW 830nm IR laser, set at 30% power and passed through a RG780 filter, on a Risø TL/OSL-DA-20 reader to stimulate feldspars. Emission for quartz was through UV340 (ultraviolet filters) and for feldspars through a blue filter pack providing transmission in the 350-450 nm range. At Witwatersrand the signal was collected for 40 seconds, with the first 0.125 seconds used for analysis and the last 16 seconds for background. At Washington for both quartz and feldspar, the signal was collected for 0.8 seconds, with the first 0.06 seconds used for analysis and the last 0.15 seconds for background. The $D_e$values are obtained by calibrating the natural signal against laboratory dose using the single-aliquot regenerative (SAR) protocol (Murray and Wintle 2000). This protocol measures the natural signal and the signal from a series of regeneration doses applied in a range to bracket the natural signal. A small test dose (5-8 Gy in this case) is used to monitor and correct for any sensitivity changes brought about by preheating, irradiation and light stimulation. Zero dose and repeat regeneration doses are used to detect aliquots of grains where the assumption of the method are not met. These are removed from analysis along with others that lack a measurable signal, have a natural signal that is too high to intersectthe regeneration growth curve and, in the case of quartz, are deemed to be feldspar by response to IR stimulation. A preheat is used in the SAR procedure to remove unstable signal. At Witwatersrand a preheat of 180°C for 10 seconds after the regeneration doses and of 160°C with no hold time (cut heat) after the test doses was used. At Washington, a preheat of 240°C and a cut heat of 200°C was used for quartz, and a preheat of 250°C for 1 minute after both regeneration and test doses was used for feldspar (unless otherwise indicated). A dose recovery test was performed on some samples. In this test, the luminescence is first removed by light exposure, a dose of known magnitude is administered, and the SAR procedure is applied to see if the known dose can be obtained.

Dose rate was determined by high resolution gamma spectroscopy at the University of Johannesburg for the Witwatersrand samples, and by thick source alpha counting, beta counting and flame photometry at Washington. Adjustments for water content were made. Cosmic dose contributions were determined following Prescott and Hutton (1994) with allowance given for the configuration of the rock shelter. Dose rate conversion followed Guerin et al. (2011). Age is calculated by dividing the D_e by the dose rate following procedures in Aitken (1985). All given error terms are computed at one-sigma.

Dose Rate

Dose rate information for the two laboratories is given in Table 1. Samples were taken from different profiles, so depth and layer number do not correlate perfectly. Using gamma spectrometry, the Witwatersrand laboratory was able to detect radon emanation in the samples. The Washington lab used alpha counting, but if the radon emanation has been more or less constant through time, alpha

194 counting, which measures activities of parents and daughters together and not concentrations of
195 particular radionuclides, should take this into account. The Washington lab also measured the beta
196 dose rate by thick source beta counting. The beta dose rate can be calculated from alpha counting
197 results (along with K concentrations) by assuming secular equilibrium. Beta counting gives a direct
198 measure of activity and a comparison between the beta dose rate from beta counting and that
199 calculated from alpha counting (including the contribution from ^{40}K), any significant disequilibrium in the
200 top of the ^{238}U decay chain in particular can be detected. For all six samples from the Washington lab,
201 the beta dose rate determined in the two ways agreed at 2-sigma, four of them at 1-sigma.

202 Moisture content was taken as measured. The lower samples were wetter than the upper
203 samples. For the Washington lab, the upper two samples were estimated to have 6 ± 3% water and the
204 lower four samples 12 ± 5%. The Witwatersrand used the measured values, given in Table 1. These are
205 broadly similar to the values used by the Washington lab.

206 The total dose rates from quartz between the two labs are broadly similar, ranging from 1.10 to
207 1.40 Gy/ka for the Witwatersrand samples and from 1.19 to 1.96 Gy/ka for the Washington samples.
208 The overlap in the ranges is even stronger if one high value from the Washington lab is removed. Given
209 that the dose rate was measured in very different ways between the two labs, this gives confidence in
210 the dose rate results. K-feldspars were also measured by the Washington lab, so the corresponding dose
211 rates are also given in Table 1. These are higher because of the contribution of internal ^{40}K within the
212 grains. This was estimated at 10 ± 3%, which is typical for relatively sensitive K-feldspar grains (Smedley
213 et al. 2012).

214 Table 1. Dose rates

University of Witwatersrand								
Sample	Depth (m)	Layer	U pre-radon (ppm)	U post-radon (ppm)	Th (ppm)	K (%)	Dose Rate (Gy/ka) quartz	Measured Water content %
MW1 (W17381)	0.3	I	1.35±0.01	0.27±0.02	2.64±0.02	0.59±0.01	1.18±0.04	7.08±2
MW2 (W17382)	0.4	I	1.81±0.01	0.36±0.01	2.67±0.01	0.72±0.01	1.31±0.04	9.55±2
MW3 (W17383)	0.5	II	1.60±0.01	0.32±0.02	3.13±0.02	0.74±0.01	1.28±0.04	14.64±2
MW4 (W17384)	0.6	II	1.38±0.01	0.28±0.01	2.40±0.01	0.89±0.01	1.40±0.04	8.36±2
MW5 (W17385)	0.8	II	1.46±0.01	0.29±0.02	2.83±0.02	0.66±0.01	1.13±0.06	18.05±2
MW6 (W17386)	1.25	IV	1.64±0.01	0.33±0.02	2.90±0.02	0.62±0.01	1.10±0.02	18.05±2
University of Washington								
Sample	Depth (m)	Layer	U (ppm)		Th (ppm)	K (%)	Dose Rate (Gy) quartz	Dose Rate (Gy) K-feldspars
MW7	0.3	I	2.34±0.15		3.36±0.75	0.41±0.02	1.19±0.06	1.74±0.17

(UW3726)							
MW8 (UW3727)	0.7	II	0.52±0.20	20.79±1.94	0.62±0.04	1.96±0.11	2.10±0.21
MW9 (UW3728)	0.8	III	1.79±0.18	12.04±1.34	0.63±0.02	1.52±0.09	1.70±0.20
MW10 (UW3729)	1.0	IV	2.60±0.17	5.19±0.86	0.57±0.02	1.41±0.08	2.03±0.20
MW11 (UW3730)	1.0	III	3.24±0.19	3.56±0.72	0.56±0.02	1.42±0.08	2.06±0.20
MW12 (UW3731)	1.1	IV	3.98±0.28	11.91±1.50	0.54±0.01	1.50±0.10	2.14±0.21

Quartz Equivalent Dose and Ages

The Witwatersrand lab performed multi-grain single aliquot OSL analysis on 48 quartz aliquots from each sample sent to that lab. Of these, between 22-40 aliquots were suitable for analysis, the others rejected where the recycling ratio of the corrected signals from two identical regeneration doses did not fall within 0.9 and 1.1 and where the recuperation of the signal from a zero dose was more than 10% of the natural signal. A dose recovery test using the 180°C preheat on 8 aliquots produced an obtained/administered ratio of 1.05±0.04 with over-dispersion of 4%. Table 2 gives the results from the natural samples. The ages from the central age model (CAM) (Galbraith and Roberts 2012) are in the right stratigraphic order. They show over-dispersion much higher than that obtained from dose recovery. This suggests the samples contain a mixture of ages. This could result from the presence of grains from decaying clasts that were not reset at the time of deposition. There could also be post-depositional migration of grains both up and down by water associated with plant growth. To deal with the first possibility, a minimum age model (MAM) (Galbraith and Roberts 2012) was applied.

Table 2. Multi-grain aliquot results

Sample	CAM D_e (Gy)	CAM age (ka)	Over-dispersion (%)	MAM D_e(Gy)	MAM age (ka)
W17381	157±14.5	133±12.9	55	50.0±8.03	42.4±6.94
W17382	175±1.27	134±9.47	32	123±2.72	93.9±3.46
W17383	187±9.16	146±8.31	28	111±9.89	86.7±8.13
W17384	210±19.0	151±14.3	51	116±3.01	82.8±3.26
W17385	230±14.6	203±14.2	36	153±12.1	128±10.8
W17386	321±28.9	293±27.8	42	192±5.22	160±6.37

The Washington lab performed single-grain OSL analysis on each sample sent to that lab. Table 3 gives the number of grains measured, those rejected for various reasons, and those accepted. Additional grains for UW3730 and UW3731 were not measured after it became clear quartz was unsuitable. The striking thing to notice in Table 3 is the large number of grains whose natural signal did not intersect the growth curve ("too high"). These rejections are mainly because the growth curve saturated at a level lower than the natural signal. It could mean the D_e is under-estimated because larger D_e values are eliminated because of this criterion.

Table 3. Single grains measured and acceptance data*

Sample	N	No signal	Too high	Other rejections	accepted	Acceptance rate (%)
UW3726	779	556	107	42	74	9.5
UW3727	873	636	105	43	89	10.2
UW3728	967	721	130	48	68	7.0
UW3729	970	703	162	27	78	8.0
UW3730	385	266	61	20	41	10.6
UW3731	294	185	63	12	34	11.6
Total	4268	3067	628	189	384	9.0

* Rejection criteria: "No signal" refers to grains that lacked a measurable signal, as judged by an error greater than 30% on the test dose or a natural signal that was not at least three standard deviations above background. "Too high" refers to grains where the natural signal was larger than the signal from the highest regeneration dose and thus did not intersect the growth curve. Other rejections include failed recycling where the ratio of the corrected signals from two identical regeneration doses did not fall within 0.8 and 1.2, recuperation where the signal from a zero dose was more than 10% of the natural signal and the decay curve showed a definite downward slope, feldspars deemed such because of loss of signal from an IRSL stimulation, and zero doses where the derived equivalent dose was not significantly different from zero.

A dose recovery test was done on 300 grains from UW3727. Of the 41 grains which gave an acceptable signal, the average ratio of obtained/administered dose was 1.11 ± 0.5, which is only slightly over-estimated. The distribution was consistent with a single value, meaning no over-dispersion. Table 4 gives D_e and age data in terms of the central age model. Because of the high over-dispersion a finite mixture model (FMM) (Galbraith and Roberts 2012) was also applied. This model divides the distribution into single-aged components assuming a Gaussian distribution and an over-dispersion value typical of a single-aged distribution. Over-dispersion values of either 0.1 or 0.15 were assumed. Results from using either did not make a significant difference. The D_e and age from the component with the largest D_e value and oldest age are also given in Table 4. FMM, not easily applied to multi-grain aliquots, addresses the structure of the D_e distribution. Grains post-depositionally moving up or down or or old grains from clast decay will affect this structure.

Table 4. Single-grain D_e and age

Sample	CAM D_e (Gy)	Over-dispersion (%)	CAM age (ka)	Largest FMM D_e (Gy) *	Proportion (%) *	FMM age (ka)
UW3726	46.5±3.28	44.1±6.4	39.1±3.51	51.3±2.56	88.8	43.2±3.2
UW3727	35.8±2.85	60.5±6.7	18.2±1.88	76.6±5.17	23.0	39.0±3.7
UW3728	42.8±2.87	37.2±6.3	28.1±2.71	58.5±3.40	62.6	38.4±3.5
UW3729	46.8±3.12	40.4±6.3	33.3±3.07	53.8±2.96	87.9	38.2±3.2
UW3730	54.5±6.0	49.4±10.2	53.8±6.09	76.5±7.25	73.9	53.7±6.1
UW3731	75.8±6.43	28.6±9.1	50.5±5.72			

* FMM divides distribution into single-aged components given an over-dispersion considered typical of a single-aged sample (10% in this case). The value given is the average age of the component with the largest D_e. An exception to this is for UW3726 where the 2nd largest component is given, because the largest contains only 2.1% of the grains. The values under "proportion" are the proportion of grains assigned to the largest FMM component. For UW3731, the total distribution is consistent with the central age value, possibly because of small sample size.

Whether using CAM or the oldest component of FMM, the single-grain ages are younger than the multi-grain single aliquot ages by at least a factor of two. A ready explanation for this is the number of grains rejected in the single-grain analysis because the natural signal was too high. These signals

were included in the multi-grain analysis and therefore would have increased the D_e. See supplementary figure showing the decay curve and growth curve of a grain where the natural signal is much higher than the signal from the highest regeneration dose. The natural signal went up and there were enough grains with higher characteristic doses to allow interpolation into the average dose response curve.

An under-estimate of D_e in older samples can occur if a fast-bleaching component begins to saturate while a medium-bleaching component does not. The under-estimation can be removed in these cases by calculating the ratio between these components (called the fast ratio) (Duller 2012, Feathers and Pagonis 2015) and eliminating grains with low fast ratios. But on these samples, D_e from grains with low fast ratios did not differ significantly for the most part from those with high fast ratios. For example, for UW3726, the central age value for grains with fast ratios greater than 6 was 49.4 ± 6.5 Gy, while for all grains it was 45.3 ± 3.2 Gy. It has also been suggested that under-estimation can be corrected by removing grains with low characteristic doses (D_o) (Thomsen et al. 2016). D_o defines the curvature of a saturating exponential used for fitting the growth curves. Looking at UW3727 in detail and considering all accepted grains plus those rejected as "too high", the D_o values averaged 35.9 ± 2.70 Gy with an over-dispersion of 59 ± 6%. A finite mixture model divided the distribution into four components, the largest, representing 66% of the grains, giving a D_o of 24.9 ± 0.79 Gy. Table 5 gives the average D_e for four ranges of D_o values, each range representing 47 grains, ordered from low to high without taking into account differential precision. The number of "too high" rejections is also given. As expected, the lower the D_o the greater number of "too high" rejections and the lower the average D_e of those accepted. But the average D_e of the grains of the third group (D_o 31-60 Gy) is not much smaller than that of the fourth group with the highest D_o values. Even considering the 10 grains with the highest D_o values, the average D_e is only about 40 Gy. The D_e values seem to be reaching a plateau for D_o values of above 30. The age for the 4th group would be 22 ± 2.6 ka, still very much an under-estimation in terms of the archaeological expectations. So removing grains with low D_o values does not improve matters. It is worth looking at a different dosimeter than quartz.

Table 5. Characteristic doses and D_e values for UW3827

Characteristic dose (Gy)	# accepted	D_e (Gy)	# "too high"*
< 21.5	9	16.8±6.40	38
21.5 - 30	16	25.9±3.90	31
31 - 60	24	41.9±4.34	23
> 61	42	43.1±4.26	5

* Defined in Table 4.

Feldspar Equivalent Dose and Age

K-feldspars, which are commonly measured using infrared stimulated luminescence (IRSL), are known to saturate at much higher levels than quartz. They also suffer from what is called anomalous fading, an athermal loss of signal that can lead to age underestimation. Fading effects can be reduced either by employing a non-fading signal or by applying a correction procedure. Both approaches are used here.

A commonly used correction procedure is that of Huntley and Lamothe (2001), which measures a fading rate using laboratory storage times (Auclair et al. 2003) and extrapolates that to ancient times using an iteration procedure. It works best for younger samples where the growth curve is in the linear region. Single-grain analysis was done. Equivalent dose is first measured on each grain and then a fading test is done also on each grain. The result is an age correction for each grain. Measurements were made on all University of Washington samples except UW3729 for which there was insufficient material. Table 6 gives the number of grains measured, those rejected for various reasons, the number of accepted grains, and the percentage of accepted to measured. The feldspars are more sensitive than the quartz (26.5% acceptance), but still suffer from a high number of grains where the natural does not intersect the growth curve. Saturation effects may not have been eliminated. Supplementary figure shows decay curves and growth curves for two grains, one where the natural signal is near saturation and one where the natural signal interpolates well below the saturation limit. Table 8 gives the equivalent dose values, g-values and corrected ages (following Huntley and Lamothe 2001). Fading rates (g-values) were highly variable. This is partly due to low precision in determining fading rates on single grains, but other work in the Washington lab has shown such fading analyses to be broadly reproducible (Feathers et al. 2019). A large proportion of grains did not yield a finite fading correction (14% of those accepted) because the measured fading rate was too high (Table 6).

The over-dispersion was much higher than the 10% assumed to be typical of a single-aged sample. The finite mixture model was applied using both 10 and 15% as the typical over-dispersion. Using either value made little difference and all subsequent discussion assumes the 10% value. UW3726, UW3730 and UW3731 divided into two components. UW 3727 and UW3728 divided into three components. The age from the most abundant component is also given in Table 7 along with the proportion of grains consistent with that component. UW3730 is a near single-aged sample and gives an age of about 70 ka. The largest component for the other samples give an age in the same range, much older than the quartz single-grain ages. Radial graphs of the age distributions are given in Supplementary material.

Table 6. Acceptance rates for K-feldspars*

Sample	n	No signal	Too high	Other rejections	Accepted	No finite fading correction	Rate (%)
UW3726	293	190	11	27	65	6	22.2
UW3727	394	180	63	53	98	9	24.9
UW3728	193	44	32	36	81	6	42.0
UW3730	393	142	105	33	113	25	28.8
UW3731	387	174	66	64	83	17	21.4
Total	**1660**	**730**	**277**	**213**	**440**	**63**	**26.5**

* Rejection criteria: "No signal" refers to grains that lacked a measurable signal, as judged by an error greater than 30% on the test dose or a natural signal that was not at least three standard deviations above background. "Too high" refers to grains where the natural signal was larger than the signal from the highest regeneration dose and thus did not intersect the growth curve. Other rejections include failed recycling where the ratio of the corrected signals from two identical regeneration doses did not fall within 0.8 and 1.2, recuperation where the signal from a zero dose was more than 10% of the natural signal and the decay curve showed a definite downward slope, and zero doses where the derived equivalent dose was not significantly different from zero.

Table 7. Equivalent dose, fading and age data – K-feldspars

Sample	n	Equivalent dose (Gy)	Average g-value (%/decade)	Corrected age (ka) Central age model	Over-dispersion (%)	Corrected age (ka) Largest component (% of grains)
UW3726	65	78.0±10.1	4.16±0.80	62.6±11.5	111±14.6	116±8.56 (76%)
UW3727	98	103.9±7.19	3.95±1.01	62.9±5.65	58.8±7.5	83.6±6.30 (67%)
UW3728	81	98.5±7.12	2.77±0.64	80.3±6.35	52.6±6.6	63.8±6.98 (50%)
UW3730	113	88.2±4.58	9.02±1.47	68.7±4.92	36.9±6.8	71.2±3.43 (96%)
UW3731	82	73.9±5.17	7.73±2.31	55.7±4.72	42.8±7.3	70.0±4.18 (72%)

Because the samples are relatively old and the growth curves are beginning to saturate, the Huntley-Lamothe procedure may be underestimating the ages. A method for correcting fading in older samples was developed by Kars et al. 2008 and enhanced by King et al. (2018). This method is based on the proposition by Huntley (2006) that rates of fading can be explained by the density and distance of recombination centers from the IRSL trap. Fading measurements like the ones used for the Huntley-Lamothe method can be used to quantify the density of recombination centers and a model for estimating the fading rate and correction has been written in R by King et al. (2018). This model was applied only to the data collected for UW3728. Only 26 grains could have their fading corrected by the model. The model could not correct for fading on 22 grains because the fading test showed a negative g-value, and on 33 other grains the model produced an infinite age. The central age for the 26 grains was 70.0 ± 10.4 ka, with 72% over-dispersion, not significantly different from the Huntley-Lamothe results. By using the uncorrected age for the ones with negative g-values (which the Huntley-Lamothe program does) and using twice the characteristic dose (which defines the shape of the saturating growth curve) as an estimate for the age of the grains where the model gives an infinite age, the central age is 86.0 ± 5.20 ka with 48% over-dispersion. Again the result does not differ significantly from the Huntley-Lamothe correction. Applying the finite mixture model, the largest component (68% of grains) gives a similar age of 83.3 ± 3.44 ka.

High temperature IRSL stimulation, which follows a low temperature stimulation, has been shown to produce a signal with little or no fading (Buylaert et al. 2012). This is called post-IR IRSL. It was attempted on all samples but UW3729. The low temperature stimulation was with IR diodes at 50°C, stimulating 100 grains at a time (to save machine time). The high temperature stimulation was with the IR laser on single-grains at 290°C. A 320°C-1 min preheat was employed. Only the high temperature stimulation was analyzed.

A fading test was conducted on the high temperature stimulation. Out of about 1000 grains measured, 165 grains yielded a signal that passed all rejection criteria. Another 168 grains had natural signals higher than a saturating growth curve. The weighted average g-value was 1.3 ± 2.8 %/decade. The median value was 1.11. This suggests little significant fading, but some grains did fade. About 27% of the grains had a fading rate significantly different from zero at one sigma, but only about 7% at two sigma. Table 8 gives the corrected (using Huntley-Lamothe methods) and uncorrected ages from post-IR IRSL from the central age model for each sample, and the over-dispersion. There are no significant differences in the central age between corrected and uncorrected values. Applying the finite mixture

368 model to the uncorrected ages, UW3726, UW3727 and UW3728 yielded three components and
369 UW3730 and UW3731 yielded two components, the latter probably the result of small sample size. The
370 final column in Table 8 gives the age for the large component and the proportion of grains consistent
371 with it.

372 Table 8. post-IR $IRSL_{290}$ results.

Sample	N	No finite fading correction	Corrected age (ka)	Over-dispersion (%)	Uncorrected age (ka)	Over-dispersion (%)	Uncorrected Age (ka) – largest component (% of grains)
UW3726	36	4	46.4±9.36	103±15.4	44.0±8.06	108±13.7	103±7.93 (44%)
UW3727	38	0	59.1±10.8	90.5±14.1	50.8±7.52	86.1±11.0	79,1±4.97 (62%)
UW3728	55	0	105±9.54	49.1±7.8	89.1±6.76	48.0±6.2	136±12.7 (49%)
UW3730	13	7	68.9±15.0	41.6±22.2	69.3±6.20	29.0±8.2	89.2±9.93 (55%)
UW3731	11	1	86.2±15.2	44.2±15.5	68.6±12.0	55.8±13.4	101±8.82 (73%)

373

374 Discussion

375 The post-IR IRSL ages from the largest component are in the same ballpark as the minimum ages
376 from the multi-grain single aliquots on quartz. It was argued earlier that the multi-grain single aliquot
377 ages may not be reliable because they represent averaging of signals among grains, quite a few of which
378 have natural signals that exceed the saturation limit of the grains. The single-grain analysis produced
379 much younger ages. The feldspars provide comparable ages to the multi-grain results but do not have
380 this reliability problem. An alternative interpretation is that the single-grain quartz ages are correct and
381 the feldspar ages represent poor bleaching. Application of the finite mixture model certainty suggests
382 the grains are of mixed-age, poor bleaching being a possible cause. One reason the samples might
383 appear partially bleached is the presence in the deposits of decaying clasts from the quartzite walls.
384 These could contribute really old grains, but the distribution of single-grain ages for both quartz and
385 feldspar samples do not suggest any really old grains, just a mixture of younger grains. The “too high”
386 signals are mainly from grains with low saturation values. The archaeological investigation (de la Peña
387 et al. 2018) suggests the allogenic sediments are largely aeolian in origin but does mention that
388 bioturbation, more visibly evident in other parts of the excavation than where these samples were
389 taken, may affect the finer grain sizes. Roots and water percolation may be the main agents in moving
390 grains vertically. While partial bleaching cannot be ruled out entirely, bioturbation and water
391 percolation seem a more likely explanation for the mixed distributions. The values of the different
392 components are also too far apart to be readily explained by microdosimetry. If partial bleaching is not
393 the case, then the quartz ages must be considered unreliable.

394 The various fading correction procedures for the feldspars give variable results, but there is
395 some consistency. Looking at the radial graphs in the supplementary material, UW3730 (using the
396 Huntley-Lamothe correction) produces a near single-aged distribution with the main component giving
397 an age of 71.2 ± 3.43 ka. This is nearly identical to the central age of the corrected postIR-IRSL result of

68.9 ± 15.0 ka, which is also single aged. The uncorrected postIR-IRSL distribution divides rather evenly into two components, but increasing the over-dispersion typical of a single-aged sample from 0.1 to 0.15, the sample becomes single-aged with an age of 69.3 ± 6.20. The ages from two different ways of dealing with fading thus converge to about 70 ka. Because this sample is near single-aged, the argument for partial bleaching also becomes less convincing. UW3728 is from the same layer (layer III) as UW3730. The radial graph shows a much more mixed sample, but the CAM from the Huntley-Lamothe correction provides an age of 80.3 ± 6.35 ka. The larger component, but with only 50% of the grains, gives an age of 63.8 ± 6.98 ka, the Kars-King correction gives an age of 70.0 ± 10.4, but with the largest component (68%) giving an age of 83.3 ± 3.44. The middle component, not the largest, of the postIR-IRSL gives an age of around 75 ka. The largest component gives a much older age. The age for this sample, then, is not as well defined as UW3730, but it is broadly consistent with it. For UW3731 (from layer IV), the radial graphs of the Huntley-Lamothe corrected distribution shows some bimodality. The largest component (72% of the grains) gives an age of 70.04 ± 4.18 ka. The CAM postIR-IRSL ages are consistent with this, but the larger component of these distributions suggest an older age of about 100ka. Again, the age of this sample is hard to pin down but it appears consistent with UW3730 or perhaps somewhat older. In sum, the lower three samples for which feldspar was measured give ages of around 70 ka, with the lowest one maybe slightly older.

The radial graph for UW3727 (Layer II) shows an evenly mixed sample. The Huntley-Lamothe corrected CAM is 62.9 ± 5.65 ka, which fits stratigraphically with the lower samples. The postIR-IRSL CAM is consistent at 50.8 ± 7.52 ka. Using the largest component in either of these gives ages of around 80 ka, which does not fit stratigraphically. UW3726 from Layer 1 is the biggest puzzle (Figure 4). The radial graph of the Huntley-Lamothe corrected distribution shows bimodality, with the oldest component giving an age of 116 ± 8.56 ka. The CAM of 62.6 ± 11.5 ka seems in the right ballpark, but looking at the radial graph, very few grains are consistent with that age. The postIR-IRSL gives a similar picture but it does break into three components. The radial graph in Figure 4 shows a middle component, the smallest of three with only 21% of grains, with an age of 58.1 ± 8.40 ka. This fits in with the other samples, but how much confidence can be placed in it, when there are so many grains younger and older, is debatable.

Figure 4. UW3726 uncorrected postIR-IRSL

Luminescence dating has long been employed in dating MSA sites in southern Africa, but complications as shown here for Mwulu's Cave are not uncommon. And even where robust studies have been reported (e.g., Jacobs et al. 2008), others have found room to question (Guérin et al. 2013, cf Jacobs and Roberts 2017). Already mentioned are the contrasting results from three different labs for sediments from Diepkloof Rock Shelter in the Western Cape (Tribolo et al. 2013, Jacobs and Roberts 2015, Feathers 2015). Part of the problem at Diepkloof was saturating quartz grains (Feathers and Pagonis 2015), but difficulties in determining the dose rate in a complicated setting was also important. The saturation level in quartz varies widely. Quartz from deposits related to the so-called Fauresmith industry, which is transitional from Early Stone Age to MSA, at Kathu Pan in South Africa produced ages as old as 450 ka (Porat et al. 2010), but quartz at similarly-aged deposits at Wonderwerk Cave in the same region of the Northern Cape was saturated (Chazan et al. 2008). Most applications have involved quartz, but one study comparing Na- and K-feldspars was carried out on Howiesons Poort deposits in Lesotho (Barré and Lamothe 2010). Porraz et al. (2018) also measured K-feldspars at "Pietersburg" deposits at Bushman Cave. The ages were about 20 ka older than those from quartz, which were done on single-grains because so many grains were saturated. The authors spectulated about why the feldspar ages might be over-estimates (dose reach, bleaching problems) but did not consider that the quartz ages might be under-estimates due to the saturation problem.

A relative chronology, taking into account the succession of characterized industries in South Africa, could perhaps reinforce or weaken the conclusions of the luminescence methodologies presented here. However, this seems highly difficult yet because the knowledge we have of the industries prior to Howiesons Poort and Still Bay is still very confusing (from a merely descriptive industrial point of view), particularly in the Eastern part of Southern Africa. In the Introduction we pointed out that Mwulu's Cave was *typologically* ascribed to the Pietersburg and that this attribution has been maintained until recently (cf. Tobias, 1949 and Wadley, 2015). Recognition of the Pietersburg, as a distinct technological tradition, has been resumed recently (Porraz et al., 2015, 2018). However, the existence of this stone tool archaeological identity seems very problematic. The Pietersburg was vaguely typologically defined at the beginning of the twentieth century and later re-identified in Mwulu's Cave and Border Cave (Cooke, Malan and Wells, 1945; Tobias, 1949, 1954; Mason, 1957; Sampson, 1972, 1974). Its characteristics, and the main items which represent and associate it, are still techno-typologically dubious (see de la Peña et al., 2018 for a thorough discussion). At this stage, it seems more a catch-all category rather than a useful archaeological entity. Even if it could be well-defined, its chronological position within the MSA is highly problematic. This is not surprising given the difficulty in chronologically circumscribing an industry when the characteristics that define it have not been agreed upon. Besides this, most of the sites attributed to the Pietersburg in South Africa were excavated in the 40-50' of the XXth century and only recently new research is being carried out with one of the main goals of stablishing a chronology for them. The sole exception for this is Border Cave, where a geochronological program has been promoted since the 70' (Grün and Beaumont 2001; Grün et al. 2003).

As discussed in de la Peña et al. (2018) Mwulu's Cave has a strong *Levallois* flake and blade production, with unifacial and bifacial pieces well documented in the sequence. The most abundant tool in the lower

layers (III-IV-V) are *Levallois* points. These technological characteristics can be compared, roughly, with the lower layers of Bushman Rock Shelter and the basal members of Border Cave (5BS, 4WA, and 5WA), which are the two sites that have been typologically compared with Mwulu's (Mason, 1957; Sampson 1972, 1974; Beaumont, 1978) and from which we have also recent dating data (Porraz et al., 2018; Grün et al. 2003). The chronological information reported here places the archaeological deposit of Mwulu's Cave around 70ka or potentially older. This roughly matches the dates from the member 4BS, 1RGBS and BC5-Fossil at Border Cave, which has been attributed to the Howiesons Poort (Grün et al. 2003), not to the MSA1/Pietersburg as expected by previous typological comparisons (Tobias, 1949, 1954; Mason, 1957; Sampson 1972,1974; Beaumont 1978). On the other hand these dates do match the upper part of the MSA sequence at Bushman Rock Shelter, which has new OSL dates between 70 and 90 ka (Porraz et al., 2018). However, at Bushman Rock Shelter the abundance of *Levallois* points is the main typological characteristic *in the base* of the sequence (lower layers); not in the upper part where the 70-90 ka new dates are coming from (see Porraz et al., 2015; Porraz et al., 2018). So in both cases there is mismatch between the dates and the technology, although the latter remains rather ill-defined.

There are numerous MSA sites in South Africa of around 70-80 ka old, although the attributions of the associated lithic industries varies notably from site to site. For example, the following lithic 'industries'/technological traditions are proposed to occur at this time period in sites across South Africa: Pietersburg, Still Bay, Indeterminate Middle Stone Age, Howiesons Poort, MSA II, Microlithic MSA, Pre Howiesons Poort and Pre-Still Bay (we have synthesized the published data with these attributions and chronologies in Table 9). Some of these site's industries have similarities with the preliminary data known from Mwulu's Cave. However, still it is not possible to build up a strong argument base on the industrial characteristics for a relative chronological comparison. Moreover, the pre-Still Bay and Howiesons Poort phase in Southern Africa remains rather murky (Table 9).

Table 9. Southern Africa MSA layers dated around 70-80ka and their industrial/archaeological attribution.

Name of the site	Layer	Chronology		Method	Industry	Publication/s
Bushman Rock Shelter	28	73±6 ka (quartz)	91±10 (feldspar)	OSL	Pietersburg	Porraz et al., (2018)
		75±6 (quartz)	97±10 feldspar)			
Blombos	CGAA CGAA CFD CFB/CFC CFB/CFC CFA CD CC CC CA BZB CAB	78.8 ± 5.6 78.9 ± 5.9 76.7 ± 4.8 68.8 ± 4.6 75.5 ± 5.0 69.7 ± 3.9 74.9 ± 4.3 72.5 ± 4.6 74.6 ± 3.9 73.3 ± 4.4 81 ± 10 66 ± 7		OSL TL 	Still Bay	Jacobs et al. (2003a,b)

	CAC CCh1 CCh1	77 ± 8 64 ± 6 79 ± 8			
Border Cave	4 BS 1 RGBS BC5 fossil 3 WA 3 BS3		ESR	Howiesons Poort	Grün et al. (2003)
Die Kelders	Layer 11 Layer 9 Layer 7	70.3 ± 5.8 79.7 ± 15.6 75.3 ± 6.8	OSL	MSA	Feathers and Bush (2000)
Diepkloof	Logan Kate/Keny	73.6 ± 2.5 70.9 ± 2.3	OSL	Still Bay/Howiesons Poort	Porraz et al., (2008) Tribolo et al., (2013)
Hollow Rock		80.0 ± 5.0 72.0 ± 4.0	OSL	Still Bay	Högberg and Larsson (2011)
Klasies River, Cave 1/1A	SAS Member Layer 22 from (Singer and Wymer excavations	70.9 ± 5.1 72.1 ± 3.4	OSL	MSA II Pre-Howiesons Poort	Feathers (2002) Jacobs et al, 2008
Klasies River Cave 2	RF Member (Deacon ex.)	71.6 ± 2.9	OSL		Jacobs et al., (2008)
Melikane	Carter Layer 6	79.5 ± 3.1	OSL	MSA	Stewart et al. (2012)
Pinnacle Point 5–6	SADBS	70.6 ± 2.3	OSL	Microlithic MSA	Jacobs (2010)
Rose Cottage	KUA LEN LEN	71.4 ± 4.2 72.5 ± 6.8 76.3 ± 14.8	OSL	Pre-Howiesons Poort	Valladas et al., (2005)
Sibudu	RGS LBG LBG2 BS	70.5 ± 2.0 72.5 ± 2.0 73.2 ± 2.3 77.3 ± 2.2	OSL	Still Bay Pre-Still Bay	Jacobs et al., (2008)

Conclusion

Dating the sediments at Mwulu's Cave has been challenging. The quartz, while of good sensitivity, appeared to saturate early. The single-grain ages, even if one can argue for partial bleaching, are much younger than the multi-grain ages. We have argued the partial bleaching is probably not likely, and the old ages from the multi-grain aliquots are the result of averaging in of natural signals that are much higher than their saturation limits and are not reliable.

Single-grain age results from the K-feldspars are older than the quartz. Fading was dealt with in various ways, but all correction or avoidance procedures produced fairly consistent results. The ages are difficult to determine, however, because of mixing of grains, probably from bioturbation and water percolation. One sample, however, appears to be near single-aged and using that as an anchor, we

519 interpreted the ages of the others. The results suggest the sequence dates from about 60-70 ka and
520 maybe a little earlier.

521 This work shows the limitation of luminescence dating of quartz from older samples. In some
522 places, like Mwulu's Cave, the saturation level is fairly low. K-feldspars produced much better results
523 (although still with many saturated grains), but mixed distributions made exact age estimates difficult.
524 For samples in this age range, however, different ways of dealing with anomalous fading produced
525 broadly similar results.

526 The results have important implications for the Archaeology of the MSA. One is that dating of MSA sites
527 is not always going to be straightforward. The complexities involved here in applying luminescence
528 dating, while informative, should recommend caution. Another is that despite difficulties, a broad age
529 range (60-70 ka or older) was obtained for an industry that typologically has been attributed to
530 Pietersburg. While this differs to some degree from other industries labeled Pieterburg and agrees with
531 other typologically different industries (Table 9), it should be clear that any progress in the chronology of
532 the MSA will depend on clarifying the technology, work that is still ongoing at Mwulu's Cave.

533

534 **Acknowledgments**

535 We thank the Shamane Magashula community for kindly giving us permission to excavate in Mwulu's
536 Cave at Portugal Farm (Limpopo, South Africa). Paloma de la Peña thanks Simon Armitage for the
537 constructive discussions in an early phase of this research.
538 This research project was conducted under the auspices of two research grants to Paloma de la Peña
539 from the DST/NRF Centre of Excellence in Palaeosciences and from the Paleontological Scientific Trust
540 (PAST). The name of the projects are: *Understanding the variability of the Pietersburg Industries: a*
541 *comparative analysis of Middle Stone Age sites from different South African biomes* and *Luminiscence*
542 *dating for the Middle Stone Age site of Mwulu's Cave*. Opinions expressed and conclusions arrived at,
543 are those of the authors and are not necessarily to be attributed to the CoE in Palaeosciences or PAST.

544

545 **Supplementary Information**

546 Figure S1. Radial graph of K-feldspar age determinations using the Huntley-Lamothe (2001) correction
547 for sample UW3726

548 Figure S2. Radial graph of K-feldspar age determinations using the Huntley-Lamothe (2001) correction
549 for sample UW3727

550 Figure S3. Radial graphs of K-feldspar age determinations using the Huntley-Lamothe (2001) correction
551 for sample UW3728.

552 Figure S4. Radial graph of K-feldspar age determinations using the Huntley-Lamothe (2001) correction
553 for sample UW3730

554 Figure S5. Radial graph of K-feldspar age determinations using the Huntley-Lamothe (2001) correction
555 for sample UW3731.

Figure S6. Decay curve for single-grain quartz grain showing saturation for sample UW3727**.**

Fifure S7. Growth curve for single-grain quartz grain showing saturation for sample UW3727.

Figure S8. Decay curve for single-grain quartz grain showing saturation for sample UW3727**.**

Figure S9. Growth curve for single-grain quartz grain showing saturation for sample UW3727.

Figure S10. Decay curve for single-grain quartz grain showing saturation for sample UW3727.

Figure S11. Growth curve for single-grain quartz grain showing saturation for sample UW3727.

REFERENCES

Aitken, M. J. (1985). *Thermoluminescence Dating*, Academic Press, London.

Auclair, M., et al. (2003). Measurement of anomalous fading for feldspar IRSL using SAR. *Radiation Measurements*, 37: 487-492.

Barré, M., Lamothe.M. (2010). Luminescence dating of archaeosediments: a comparison of K-feldspar and plagioclase IRSL ages. *Quaternary Geochronology* 5:324-328.

Beaumont, P.B. (1978). *Border Cave*. M.A. thesis, University of Cape Town.

Buylaert, J. P., Jain, M., Murray, A. S., Thomsen, K. J., Thiel, C., Sohbati, R. (2012). A robust feldspar luminescence dating method for Middle and Late Pleistocene sediments. Boreas 41:435-451.

Chazan, M., Ron, H, Matmore, A., Porat, N., Goldberg, P., Yates,R., Avery, M., Sumner, A., Kolskal Horwitz, L. (2008). Radiometric dating of the Earlier Stone Age sequence in Excavation I at Wonderwerk Cave, South Africa: preliminary results. *Journal of Human Evolution* 55: 1-11.

Cooke H.B.S; Malan, B.D., Wells, L.H. (1945). Fossil man in the Lebombo Mountains, South Africa: the 'Border Cave', Ingwavuma District, Zululand. *Man*, 45:6–13.

de la Peña, P., Val, A., Stratford, D.J., Colino, F., Esteban, I., Fitchett, J.M., Hodgskiss, T., Matembo, J. , Moll, R. (2018). Revisiting Mwulu's Cave: new insights into the Middle Stone Age in the southern African savanna biome. *Archaeological and Anthropological Sciences* : 1-28. https://doi.org/10.1007/s12520-018-0749-9.

Duller, G. A. T. (2012). Improving the accuracy and precision of equivalent doses determined using the optically stimulated luminescence signal from single grains of quartz. *Radiation Measurements*, 47, 770-777.

Feathers, J.K. 2002. "Luminescence dating in less than ideal conditions: case studies from Klasies River main site and Duinefontein, South Africa." Journal of Archaeological Science 29: 177–194.

Feathers, J. K. (2015). Luminescence dating at Diepkloof Rock Shelter–new dates from single-grain quartz. *Journal of Archaeological Science*, 63, pp.164-174.

Feathers, J.K. and D.A. Bush. (2000). Luminescence dating of Middle Stone Age deposits at Die Kelders. *Journal of Human Evolution*, 38: 91–119.

590 Feathers, J. K., More, G., Solis, P., Burkholder, J. E. (2019). IRSL dating of rocks and sediments from
591 desert geoglyphs in coastal Peru. *Quaternary Geochronology*, 49: 177-183.

592 Feathers, J.K., Pagonis, V. (2015). Dating Quartz Near Saturation – Simulations and Application at
593 *Archaeological Sites in South Africa and South Carolina*. *Quaternary Geochronology*, 30 (Part B): 416-
594 421.

595 Galbraith, R. F., Roberts, R. G. (2012). Statistical aspects of equivalent dose and error calculation and
596 display in OSL dating: an overview and some recommendations. *Quaternary Geochronology*, 11:1-27.

597 Guérin, G., Murray, A. S., Jain, M., Thomsen, K. J., Mercier, N. (2013). How confident are we in the
598 chronology of the transition between Howieson's Poort and Still Bay. *Journal of Human Evolution*, 64:
599 314-317.

600 Goodwin, A.J.H, van Riet Lowe, C.P (1929). The Stone Age Cultures of South Africa. Annals of the South
601 African Museum, Cape Town, pp 27.

602 Grün, R, Beaumont, P. (2001). Border cave revisited: a revised ESR chronology. *Journal of Human*
603 *Eviolution*, 40:467–482

604 Grün, R., Beaumont, P.B., Tobias, P.V., Eggins, S. (2003). On the age of Border Cave 5 human mandible
605 *Journal of Human Eviolution*, 45:155–167.

606 Guérin, G., Mercier, N., and Adamiec, G. (2011). Dose-rate conversion factors: update. Ancient TL 29:5-
607 8.

608 Högberg, A., Larsson, L.(2011). Lithic technology and behavioural modernity: new results from the Still
609 Bay site, Hollow Rock Shelter, Western Cape Province, South Africa. *Journal of Human Evolution* , 61:
610 133–155.

611 Huntley, D. J. (2006). An explanation of the power-law decay of luminescence. *Journal of Physics:*
612 *Condensed Matter*, 18:1359-1365.

613 Huntley, D. J., Lamothe, M. (2001). Ubiquity of anomalous fading in K-feldspars, and measurement and
614 correction for it in optical dating. *Canadian Journal of Earth Sciences*, 38:1093-1106.

615 Jacobs, Z. 2010. An OSL chronology for the sedimentary deposits from Pinnacle Point Cave 13B. A
616 punctuated presence. *Journal of Human Evolution*, 59: 289–305.

617 Jacobs, Z., and Roberts, R. G., (2017). Single-grain OSL chronologies for the Still Bay and Howieson's
618 Poort industries and the transition between them: further analyses and statistical modelling. *Journal of*
619 *Human Evolution*, 107:1-13.

620 Jacobs, Z., Roberts, R.G., Galbraith, R.F., Deacon, H.J., Grün, R., Mackay, A., Mitchell, P., Vogelsang, R.,
621 Wadley, L., 2008. Ages for the Middle Stone Age of southern Africa: implications for human behavior
622 and dispersal. *Science*, 322(5902), pp.733-735.

623 Jacobs, Z., G.A.T. Duller and A.G. Wintle. 2003a. Optical dating of dune sand from Blombos Cave, South
624 Africa: II — single grain data. *Journal of Human Evolution*, 44: 613–625

625 Jacobs, Z., A.G. Wintle and G.A.T. Duller. 2003b. Optical dating of dune sand from Blombos Cave, South
626 Africa: I — multiple grain data. *Journal of Human Evolution*, 44: 599–612.

Jacobs Z, Roberts RG (2015) An improved single grain OSL chronology for the sedimentary deposits from Diepkloof Rockshelter, Western cape, South Africa. *Journal of Archaeological Science*, 63: 175–192.

Kars, R. H., Wallina, J., and Cohen, K.M. (2008). A new approach towards anomalous fading correction for feldspar IRSL datuing – tests on samples in field saturation. *Radiation Measurements*, 43:786-790

King, G. E., Barrow, C., Roberts, H. M., aPearce, N. J. G. (2018). Age determination using feldspar: evaluating fading-correction model performance. *Radiation Measurements*, 119:58-73.

Mason, R.J. (1957). The Transvaal Middle Stone Age and statistical analysis. *South African Archaeological Bulletin*, 12 (48):119–137.

Murray, A. S., Wintle, A. G. (2000). Luminescence dating of quartz using an improved single-aliquot regenerative-dose protocol. *Radiation Measurements*, 32:57-73.

Porat, N., Chazari, M,Grün, R., Aubert, M., Eisenmarnn, V, Kolskal Horwitrz, L. (2010). New radiometric ages for the Fauresmith industry from Kathu Pan, southern Africa: implications for the Ealier to Middle Stone Age transition. *Journal of Archaeologial Science*, 37:269-283.

Porraz, G., P.-J. Texier, J.-P. Rigaud, J. Parkington, C. Poggenpoel , D. Roberts. (2008). First characterization of an MSA lithic assemblage stratified between Still Bay and Howiesons Poort sub-stages at Diepkloof Rock Shelter (Western Province, South Africa). *South African Archaeological Society Goodwin Series*, 10: 105–121.

Porraz, G., et al. (2015). Bushman Rock Shelter (Limpopo, South Africa): a perspective from the edge of the Highveld. South African Archaeol Bull 70:166–179

Porraz G,et al. (2018). The MIS5 Pietersburg at '28' Bushman Rock Shelter, Limpopo Province, South Africa. *PloS One*, *13*(10), p.e0202853.

Prescott, J. R., Hutton, J. T. (1994). Cosmic ray contributions to dose rates for luminescence and ESR dating: large depths and long time durations. *Radiation Measurements*, 23:497-500.

Sampson, C. G. (1972). *The Stone Age industries of the Orange River Scheme and South Africa* (No. 6). National Museum Bloemfontein.

Sampson, C. G. (1974). *The Stone Age archaeology of southern Africa*. Studies in Archaeology, Academic Press.

Söhnge, P. G., Visser, D. J. L., Van Riet Lowe, C. (1937). *The Geology and Archaeology of the Vaal River Basin*. Memoirs of the Geological Survey of the Union of South Africa, 35, Pretoria.

Stewart, B., A.G. Parker, G. Dewar, M. Morley , Allott, L.(in press). "Follow the Senqu: Maloti-Drakensberg paleoenvironments and implications for early human dispersals into mountain systems." In Africa from MIS6-2: Population Dynamics and Paleoenvironments, Edited by S. Jones and B.A. Stewart. Dordrecht: Springer.

Thackeray, A.I., (1992). The Middle Stone Age south of the Limpopo River. *Journal of World Prehistory*, *6*(4), pp.385-440.

Thomsen, K. J., Murray, A. S., Buylaert, J. P., Jain, M., Hansen, J. H., Aubry, T. (2016). Testing single-grain quartz OSL methods using sediment samples with independent age control from the Bordes-Fitte rockshelter (Roches d'Abilly site, central France). *Quaternary Geochronology* 31, 77-96.

Tobias, P.V. (1949). The excavation of Mwulu's cave, Potgietersrust district. *South African Archaeological Bulletin*, 4(13):2–13.

Tobias, P.V. (1954) Climatic fluctuations in the Middle Stone age of South Africa, as revealed in Mwulu's cave. Trans Roy Soc S Afr 34(2):325–334.

Tribolo, C. et al. (2013). OSL and TL dating of the Middle Stone Age sequence at Diepkloof Rock Shelter (South Africa): a clarification. *Journal of Archaeological Science*, 40(9), pp.3401-3411.

Valladas, H., L. Wadley, N. Mercier, L. Froget, C. Tribolo, J.-L. Reyss and J.-L. Joron. (2005). Thermoluminescence dating on burnt lithics from Middle Stone Age layers at Rose Cottage Cave. *South African Journal of Science* 101: 169–174

Volman, T. P. (1981). *The Middle Stone Age in the southern Cape*. Unpublished PhD thesis: University of Chicago.

Wadley, L. (2015). Those marvellous millennia: the Middle Stone Age of southern Africa. *Azania* 50:155–226.

Wurz, S. (2013). Technological trends in the Middle Stone Age of South Africa between MIS 7 and MIS 3. *Current Anthropology*, 54(S8), pp.S305-S319.

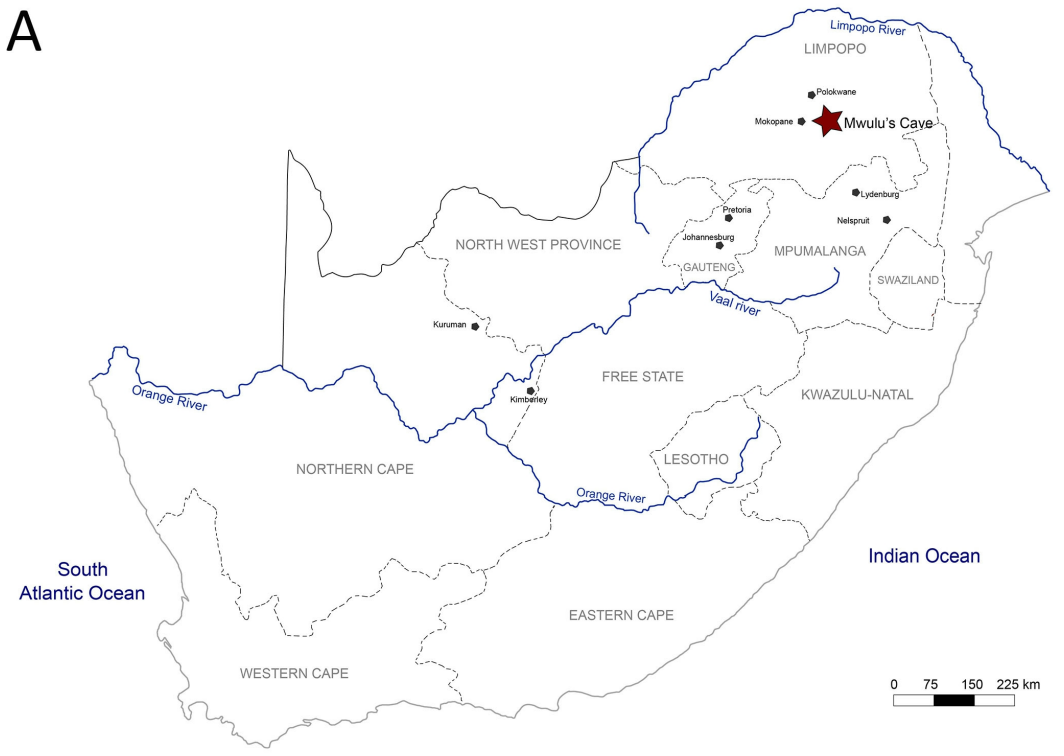
A
Limpopo River
LIMPOPO
Polokwane
Mokopane
Mwulu's Cave
Lydenburg
Pretoria
Nelspruit
Johannesburg
NORTH WEST PROVINCE
MPUMALANGA
GAUTENG
SWAZILAND
Vaal river
Kuruman
Orange River
FREE STATE
Kimberley
KWAZULU-NATAL
NORTHERN CAPE
LESOTHO
Orange River
South
Atlantic Ocean
Indian Ocean
EASTERN CAPE
WESTERN CAPE
0 75 150 225 km

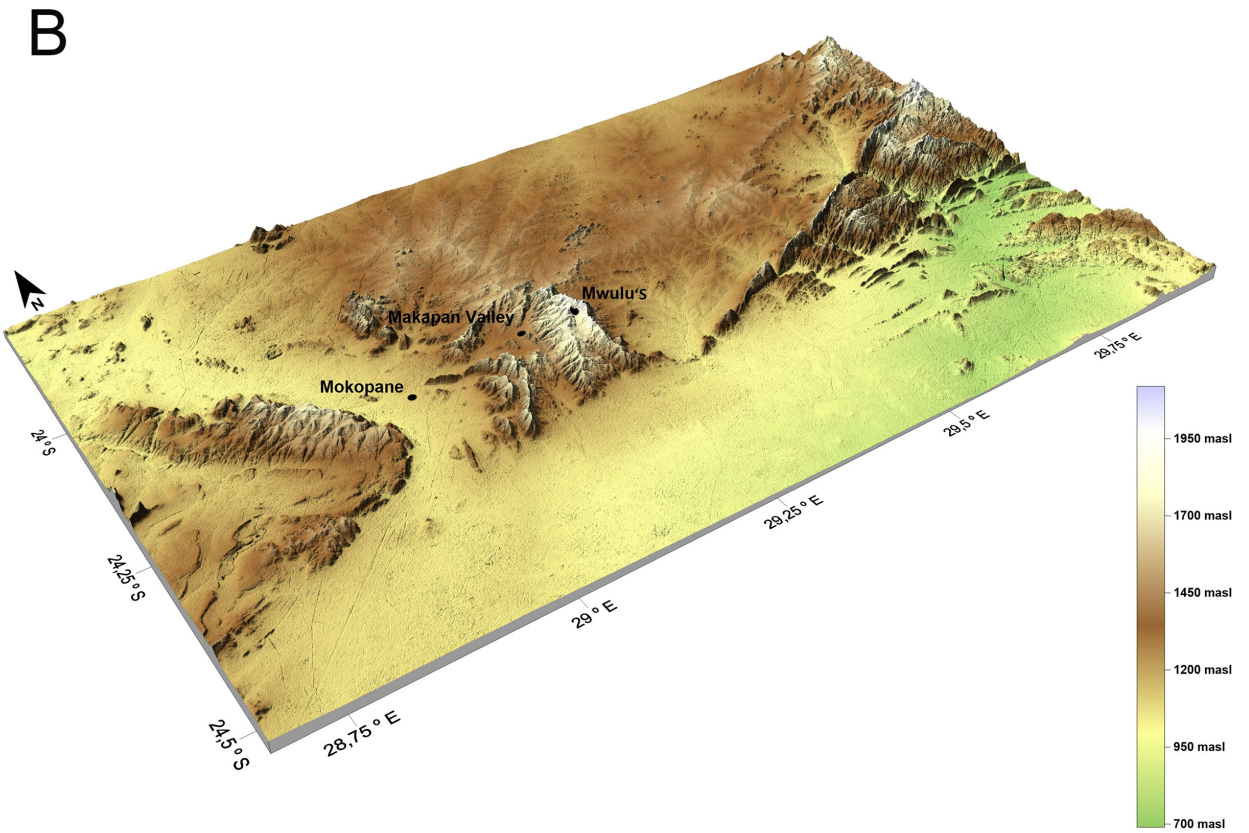
B
N
Mwulu's
Makapan Valley
Mokopane
24,0° S
24,25° S
24,5° S
28,75° E
29° E
29,25° E
29,5° E
29,75° E
1950 masl
1700 masl
1450 masl
1200 masl
950 masl
700 masl

A

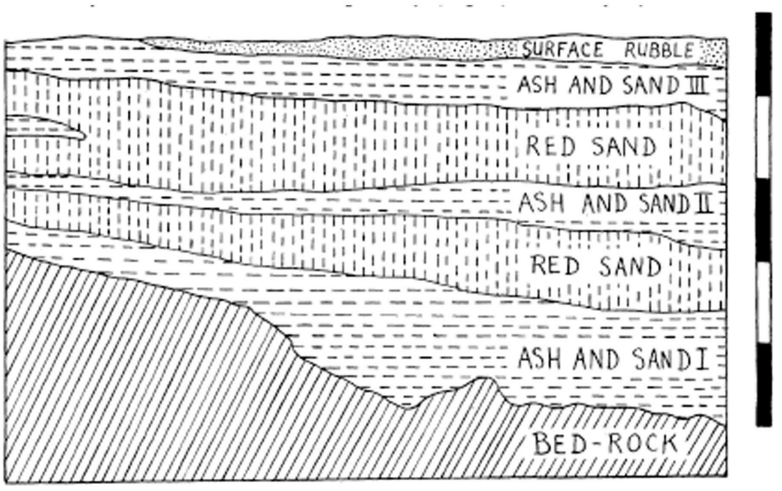

Tobias (1949)

Tobias (1949);
Tobias (1954)

de la Peña
et al.(2018)

B

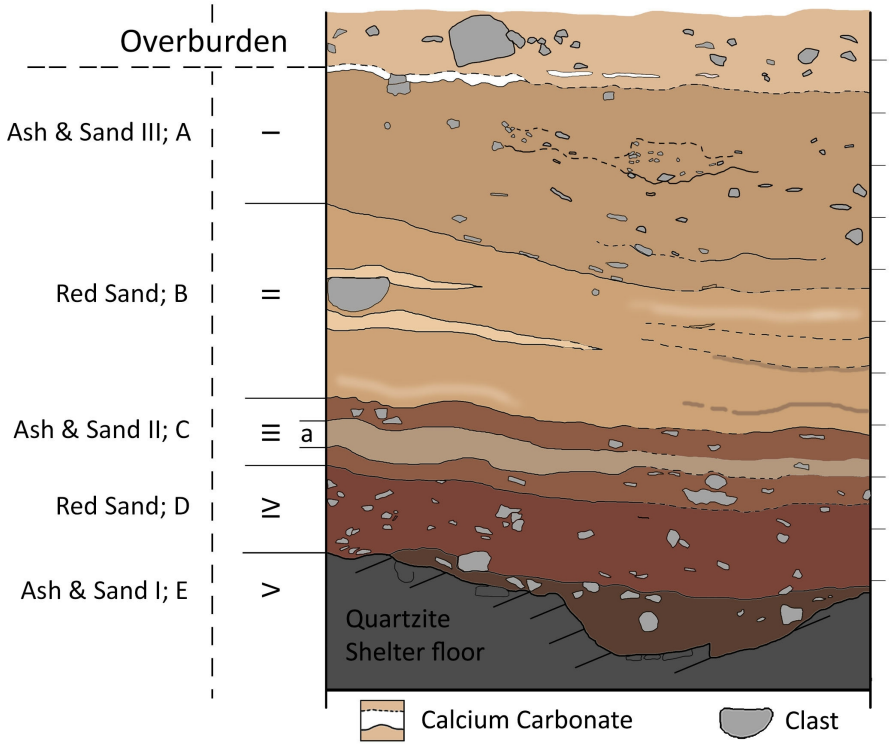

I - brown, diffuse dark and light lenses, abundant burnt & unburnt roots. Low clast & medium artefact abundance.

II - brown, diffuse dark & light lenses, burnt & unburnt roots. Low clast & low artefact abundance.

III - dark brown, burnt roots, charcoal. Low clast & high artefact abundance.

IV - brown red, roots. Low clast & high artefact abundance.

V - Very dark brown, roots. High clast & decreasing artefact abundance at the base.

WEST PROFILE

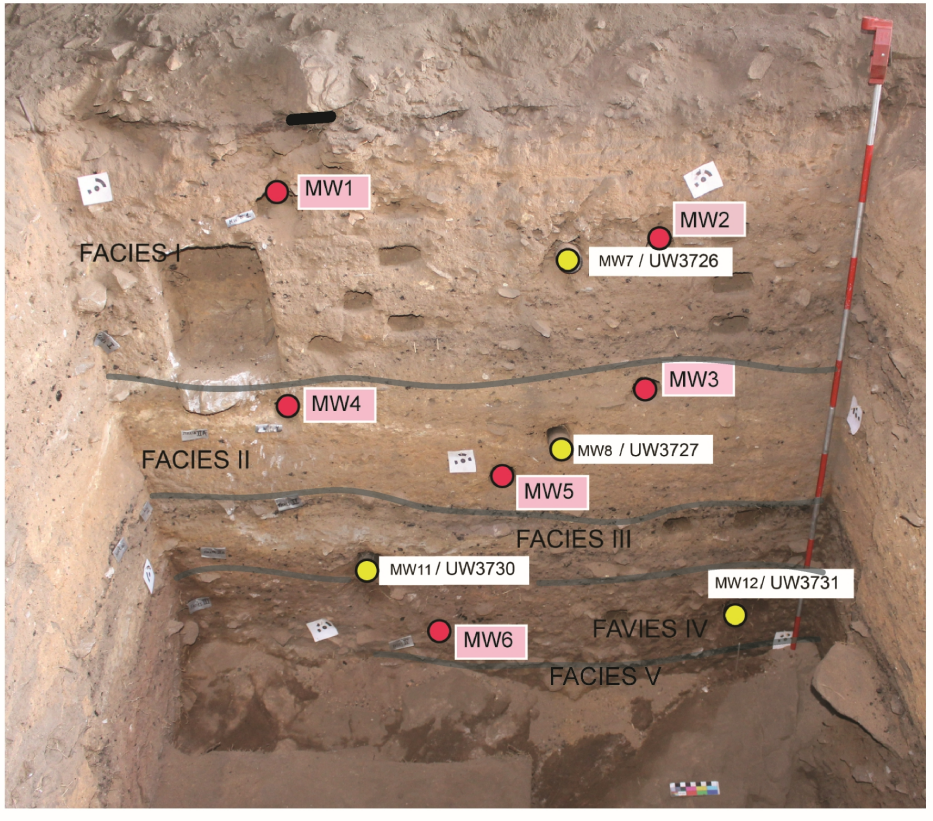

NORTH PROFILE

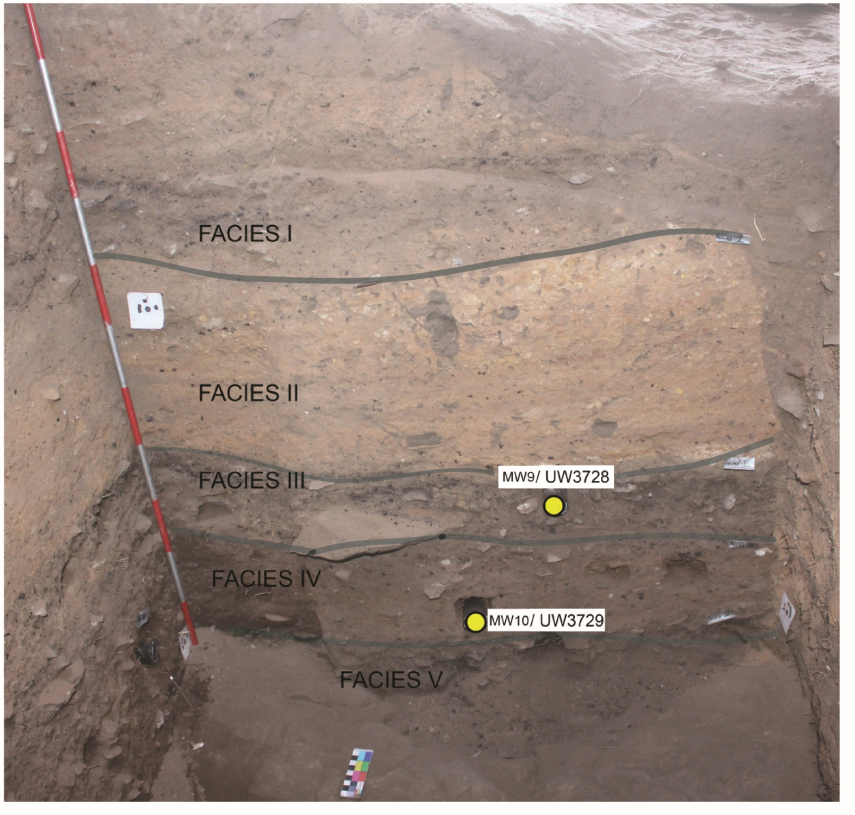

SAMPLES SENT TO WITS LAB

SAMPLES SENT TO UW LAB

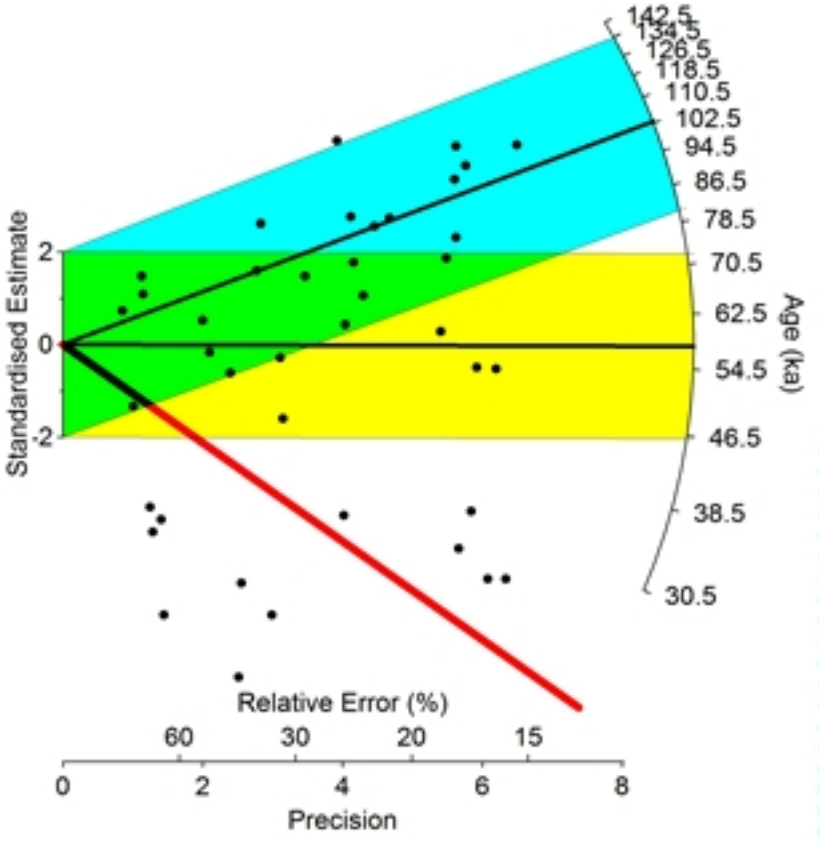
Standardised Estimate
2
0
-2
142.5
134.5
126.5
118.5
110.5
102.5
94.5
86.5
78.5
70.5
62.5
54.5
46.5
38.5
30.5
Age (ka)
Relative Error (%)
60
30
20
15
0
2
4
6
8
Precision

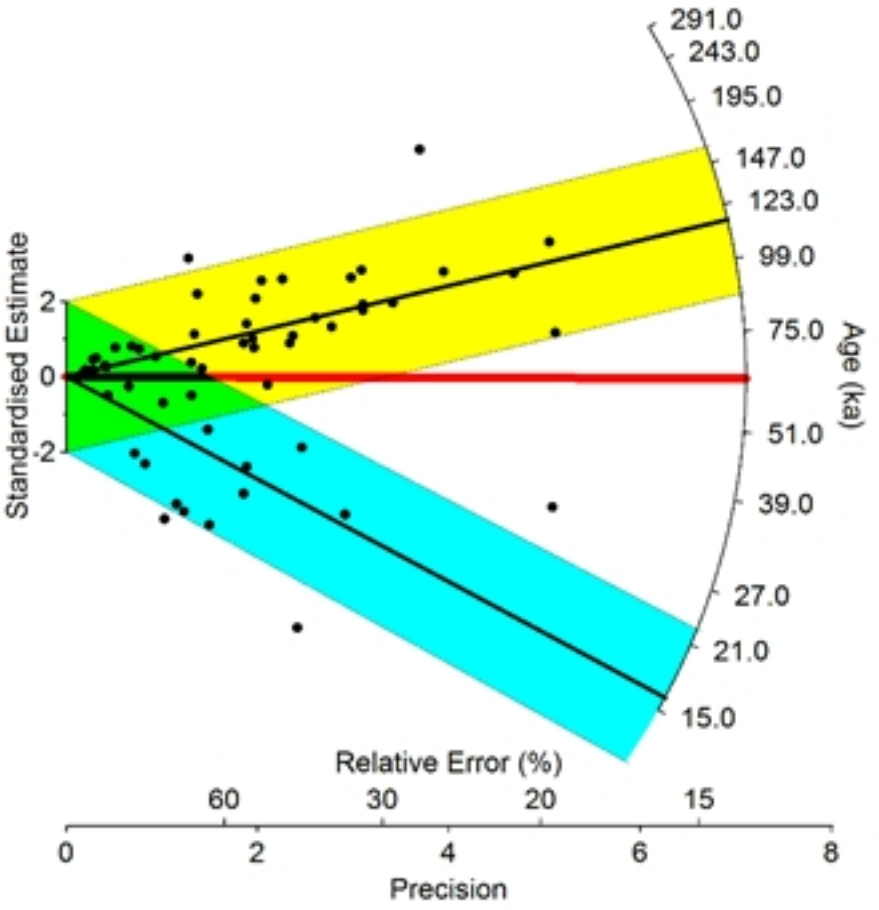
291.0
243.0
195.0
147.0
123.0
99.0
75.0
51.0
39.0
27.0
21.0
15.0
Age (ka)
Standardised Estimate
2
0
-2
Relative Error (%)
60
30
20
15
0
2
4
6
8
Precision

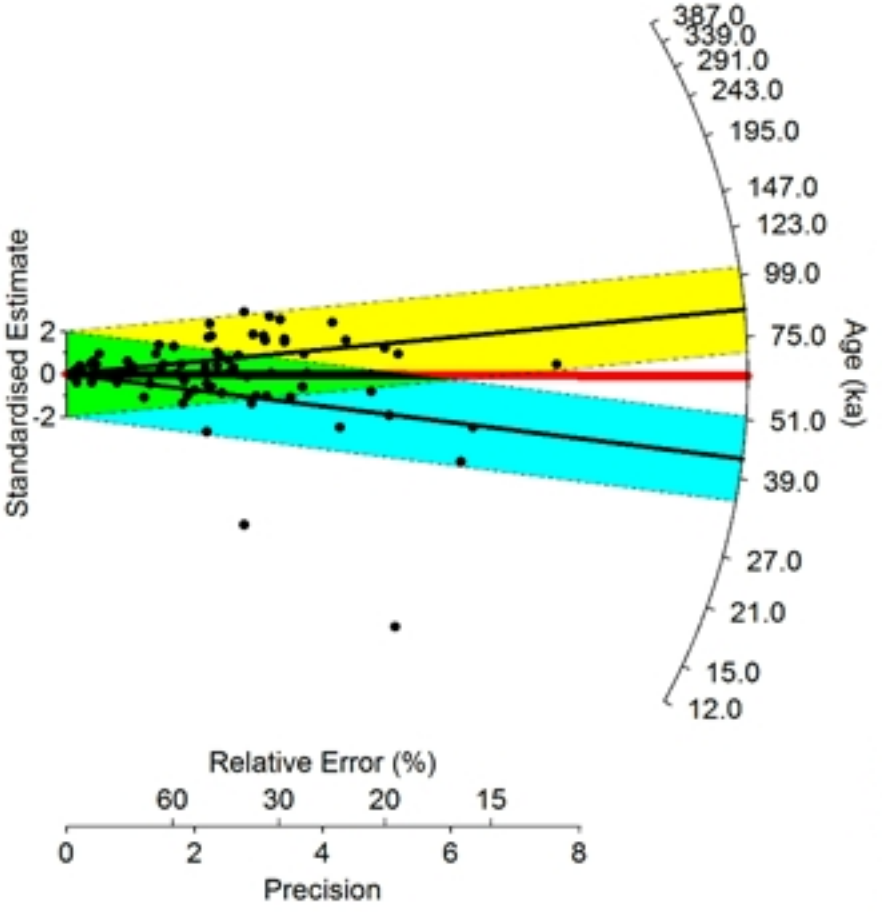
Standardised Estimate
2
0
-2
387.0
339.0
291.0
243.0
195.0
147.0
123.0
99.0
75.0
51.0
39.0
27.0
21.0
15.0
12.0
Age (ka)
Relative Error (%)
60
30
20
15
0
2
4
6
8
Precision

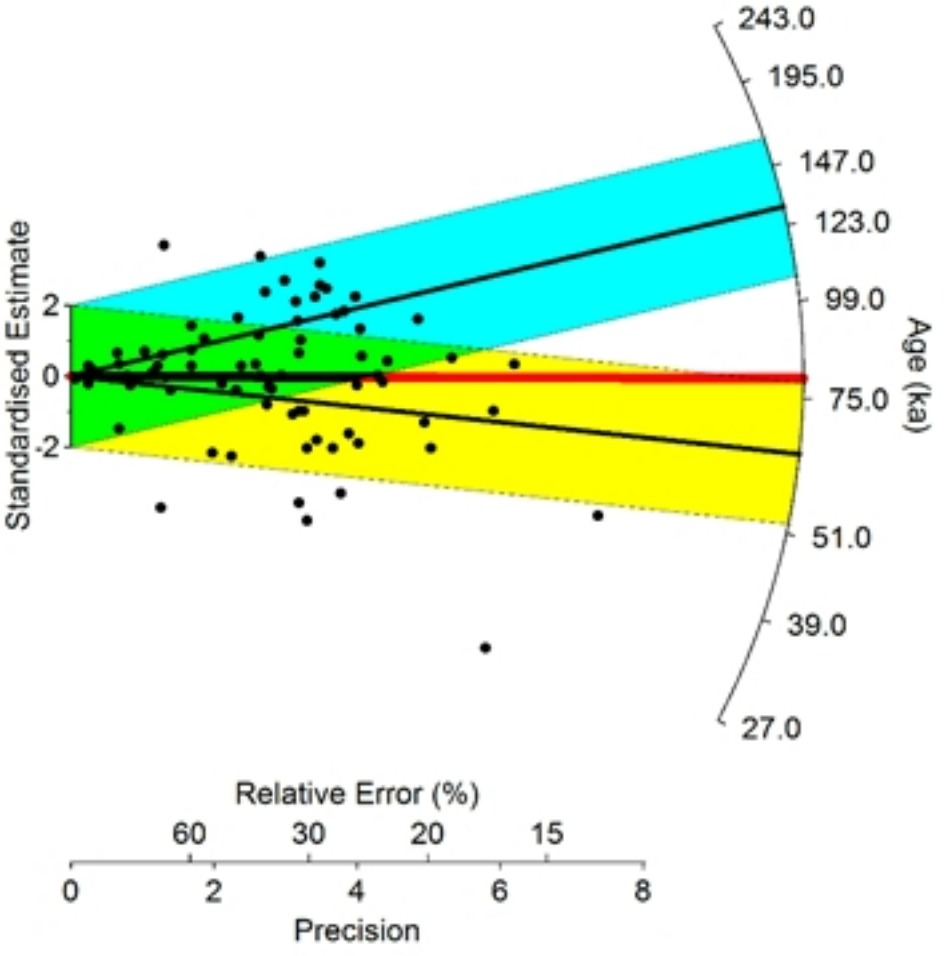
243.0
195.0
147.0
123.0
99.0
75.0
51.0
39.0
27.0
Age (ka)
Standardised Estimate
2
0
-2
Relative Error (%)
60
30
20
15
0
2
4
6
8
Precision

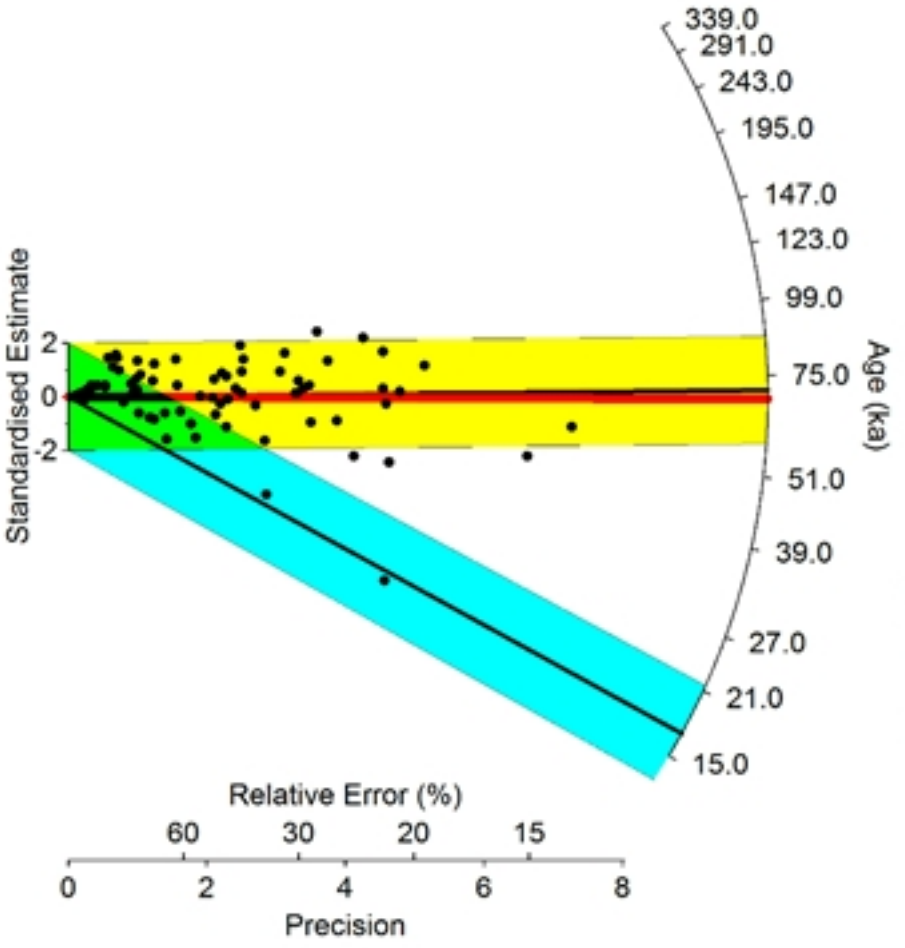
339.0
291.0
243.0
195.0
147.0
123.0
99.0
75.0
51.0
39.0
27.0
21.0
15.0
Age (ka)
Standardised Estimate
2
0
-2
Relative Error (%)
60
30
20
15
0
2
4
6
8
Precision

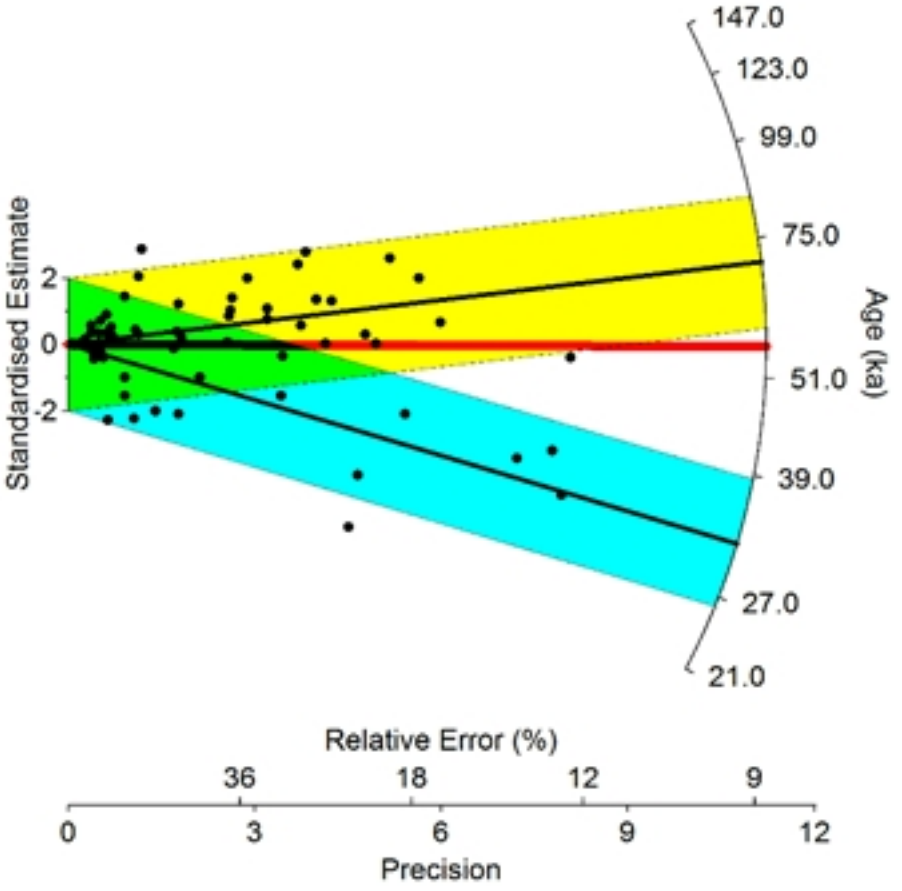
147.0
123.0
99.0
75.0
51.0
39.0
27.0
21.0
Age (ka)
Standardised Estimate
2
0
-2
Relative Error (%)
36
18
12
9
0
3
6
9
12
Precision

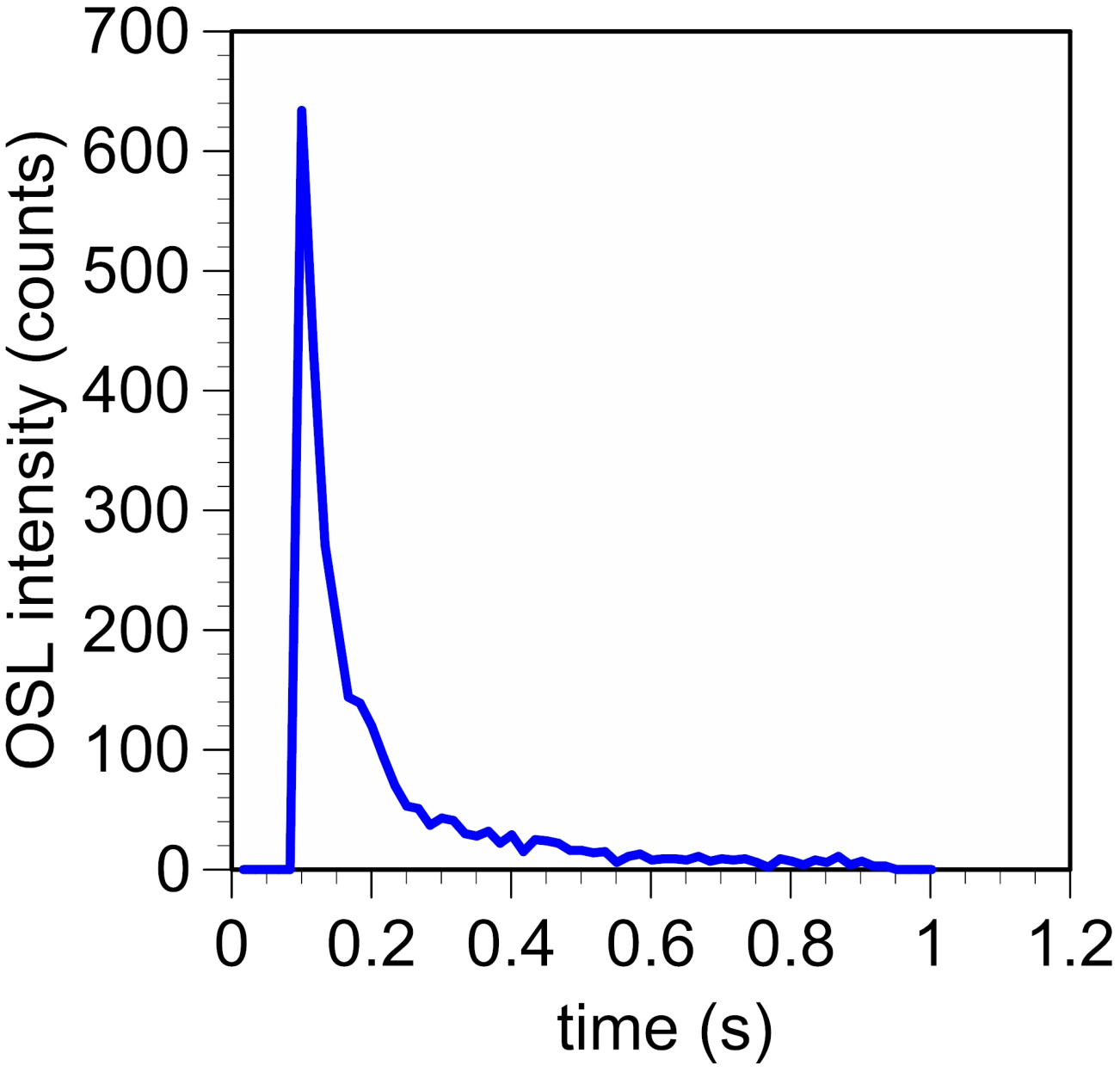
700
600
500
400
300
200
100
0
OSL intensity (counts)
0
0.2
0.4
0.6
0.8
1
1.2
time (s)

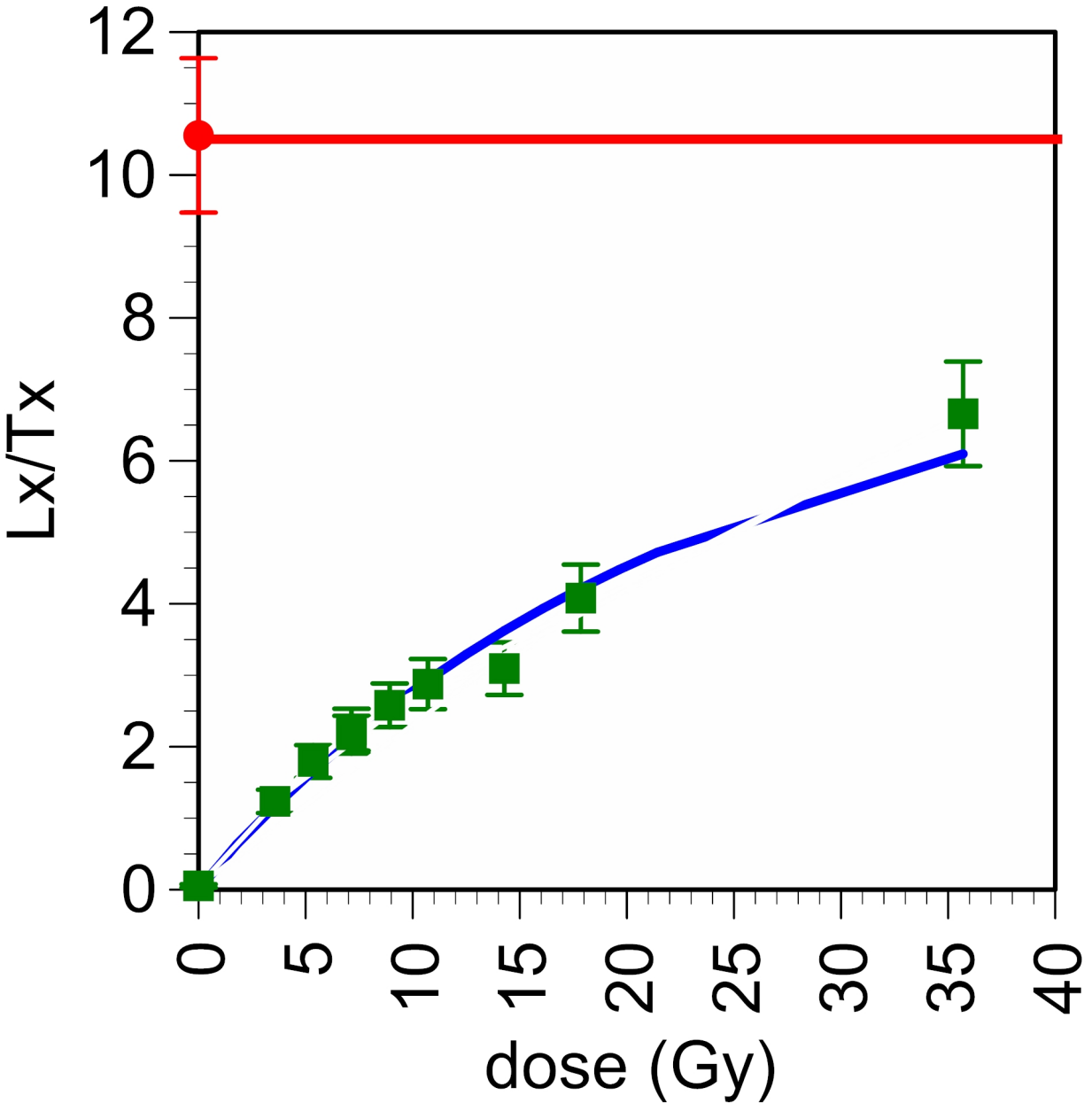
12
10
8
6
4
2
0
Lx/Tx
0
5
10
15
20
25
30
35
40
dose (Gy)

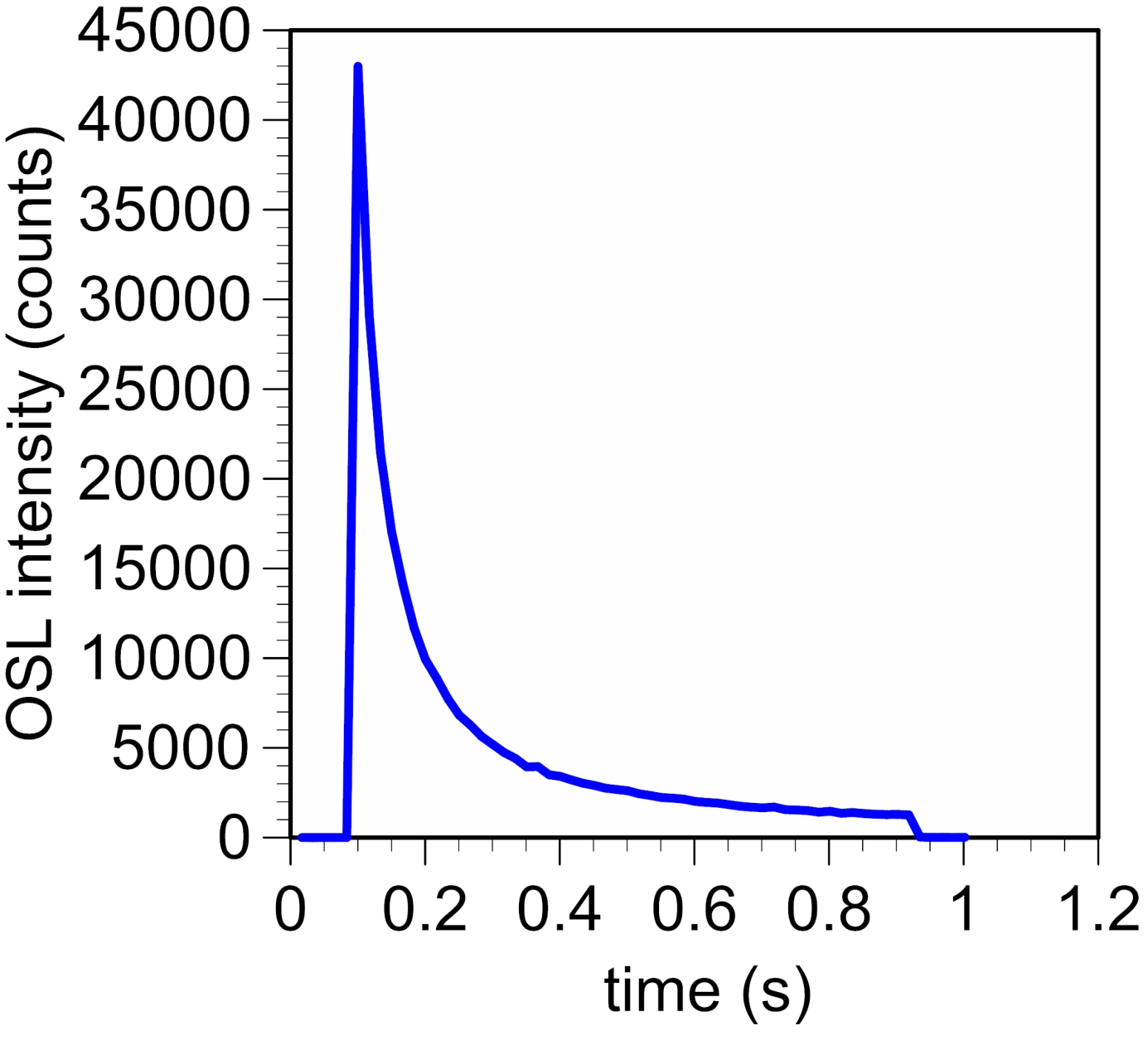
45000
40000
35000
30000
25000
20000
15000
10000
5000
0
OSL intensity (counts)
0
0.2
0.4
0.6
0.8
1
1.2
time (s)

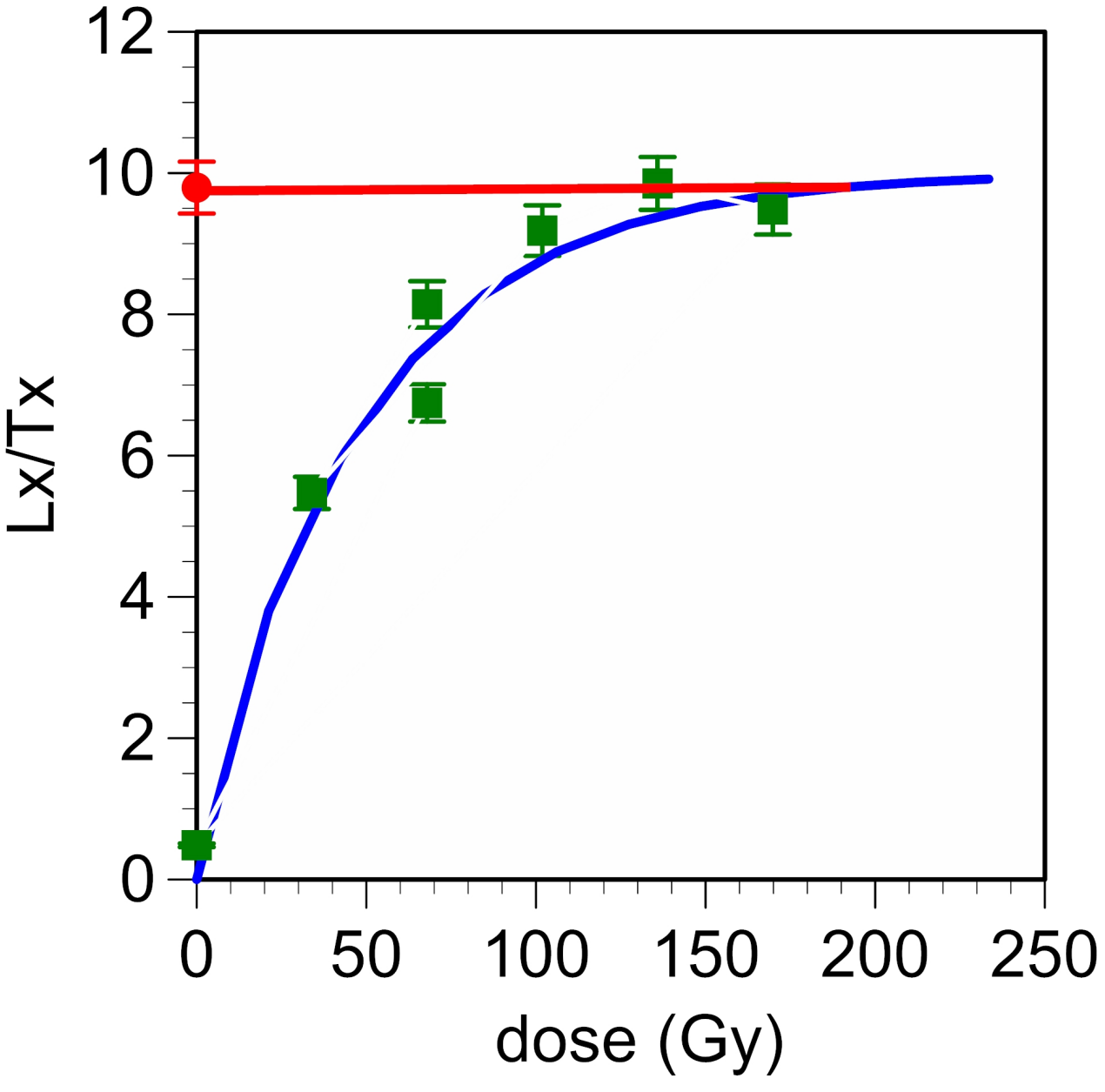
12
10
8
6
4
2
0
Lx/Tx
0
50
100
150
200
250
dose (Gy)

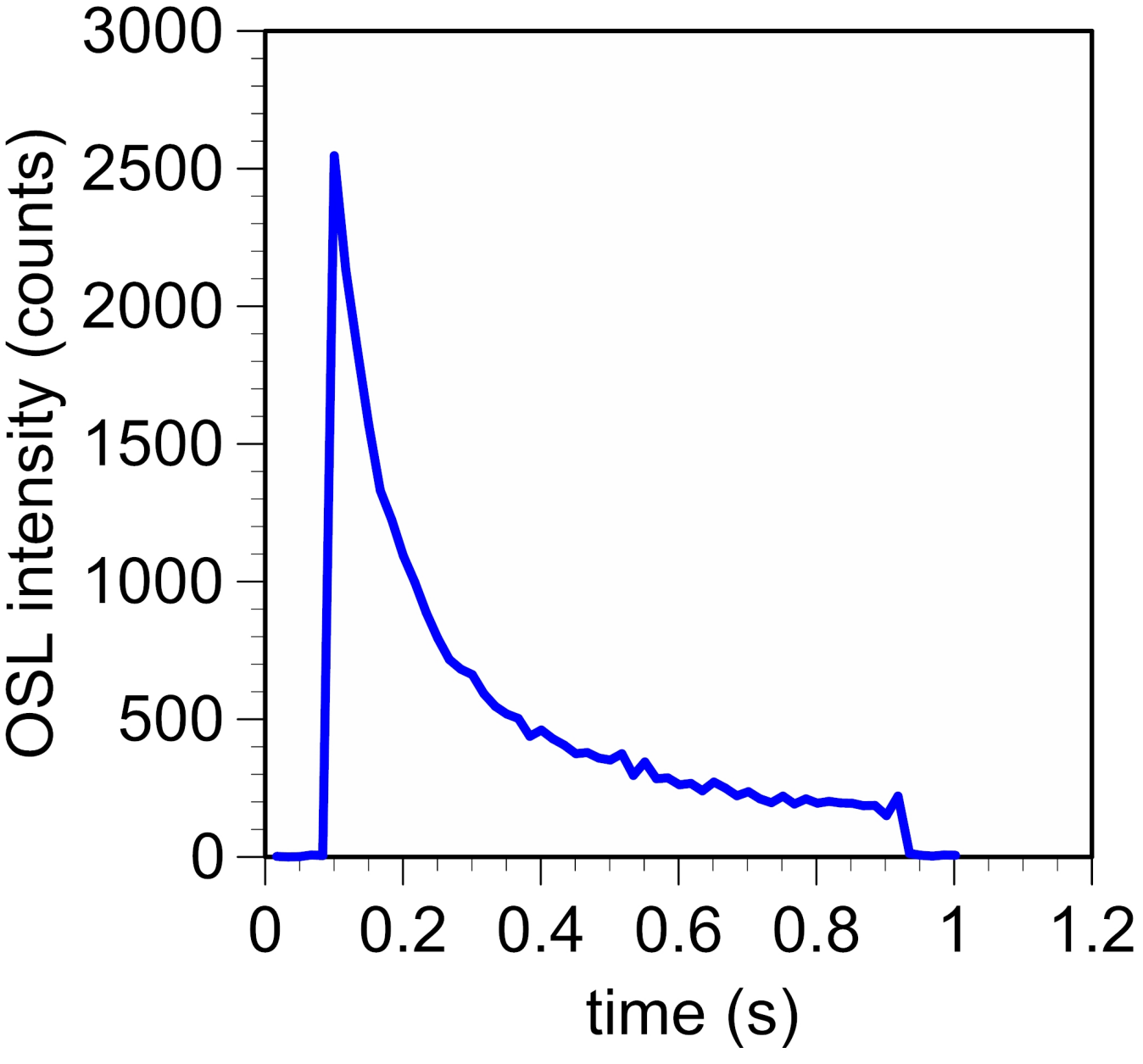
3000
2500
2000
1500
1000
500
0
OSL intensity (counts)
0
0.2
0.4
0.6
0.8
1
1.2
time (s)

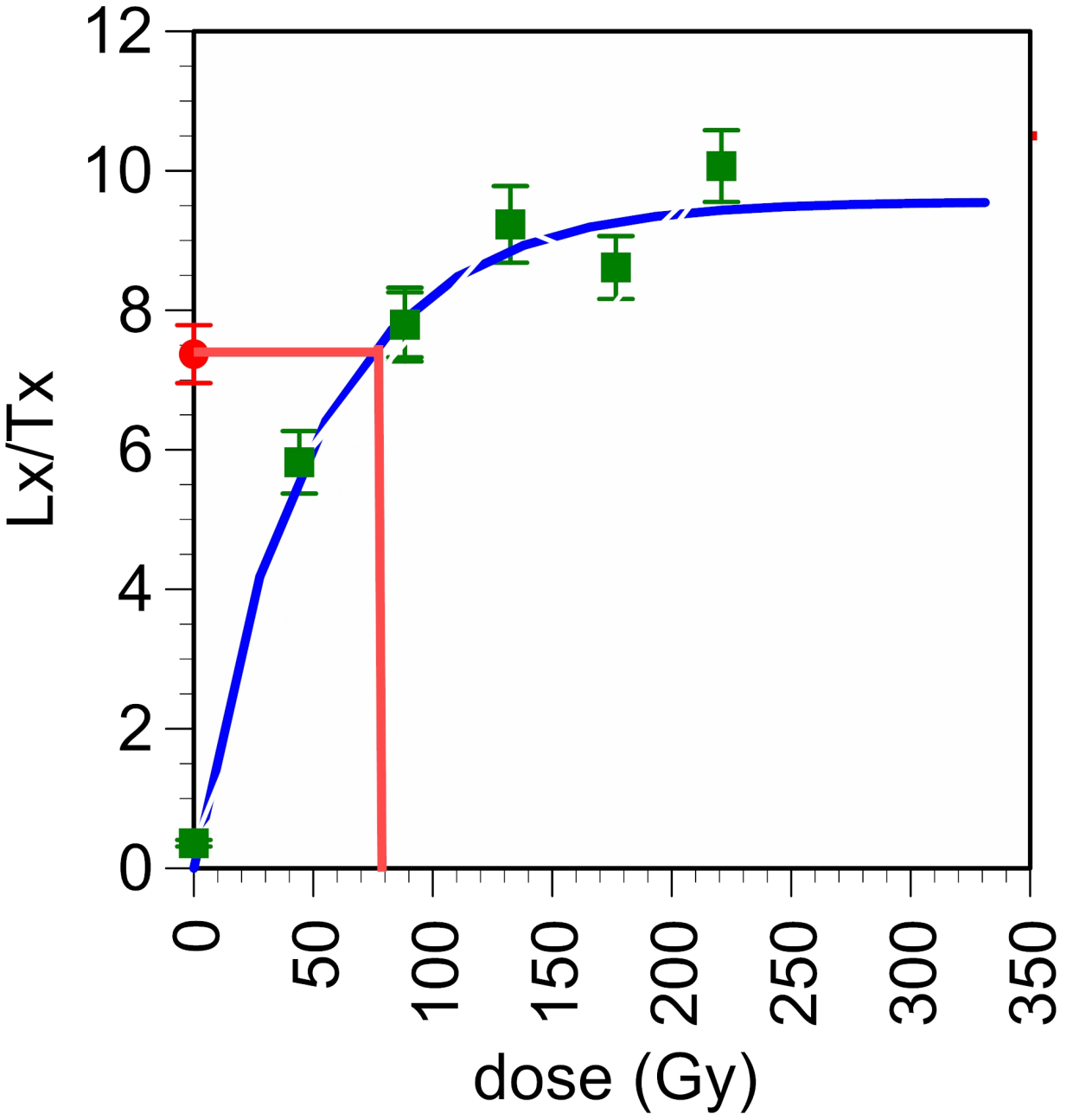
12
10
8
6
4
2
0
Lx/Tx
0
50
100
150
200
250
300
350
dose (Gy)

Table 1. Dose rates

University of Witwatersrand								
Sample	Depth (m)	Layer	U pre-radon (ppm)	U post-radon (ppm)	Th (ppm)	K (%)	Dose Rate (Gy/ka) quartz	Measured Water content %
MW1 (W17381)	0.3	I	1.35±0.01	0.27±0.02	2.64±0.02	0.59±0.01	1.18±0.04	7.08±2
MW2 (W17382)	0.4	I	1.81±0.01	0.36±0.01	2.67±0.01	0.72±0.01	1.31±0.04	9.55±2
MW3 (W17383)	0.5	II	1.60±0.01	0.32±0.02	3.13±0.02	0.74±0.01	1.28±0.04	14.64±2
MW4 (W17384)	0.6	II	1.38±0.01	0.28±0.01	2.40±0.01	0.89±0.01	1.40±0.04	8.36±2
MW5 (W17385)	0.8	II	1.46±0.01	0.29±0.02	2.83±0.02	0.66±0.01	1.13±0.06	18.05±2
MW6 (W17386)	1.25	IV	1.64±0.01	0.33±0.02	2.90±0.02	0.62±0.01	1.10±0.02	18.05±2
University of Washington								
Sample	Depth (m)	Layer	U (ppm)		Th (ppm)	K (%)	Dose Rate (Gy) quartz	Dose Rate (Gy) K-feldspars
MW7 (UW3726)	0.3	I	2.34±0.15		3.36±0.75	0.41±0.02	1.19±0.06	1.74±0.17
MW8 (UW3727)	0.7	II	0.52±0.20		20.79±1.94	0.62±0.04	1.96±0.11	2.10±0.21
MW9 (UW3728)	0.8	III	1.79±0.18		12.04±1.34	0.63±0.02	1.52±0.09	1.70±0.20
MW10 (UW3729)	1.0	IV	2.60±0.17		5.19±0.86	0.57±0.02	1.41±0.08	2.03±0.20
MW11 (UW3730)	1.0	III	3.24±0.19		3.56±0.72	0.56±0.02	1.42±0.08	2.06±0.20
MW12 (UW3731)	1.1	IV	3.98±0.28		11.91±1.50	0.54±0.01	1.50±0.10	2.14±0.21

Table 2. Multi-grain aliquot results

Sample	CAM D_e (Gy)	CAM age (ka)	Over-dispersion (%)	MAM D_e(Gy)	MAM age (ka)
W17381	157±14.5	133±12.9	55	50.0±8.03	42.4±6.94
W17382	175±1.27	134±9.47	32	123±2.72	93.9±3.46
W17383	187±9.16	146±8.31	28	111±9.89	86.7±8.13
W17384	210±19.0	151±14.3	51	116±3.01	82.8±3.26
W17385	230±14.6	203±14.2	36	153±12.1	128±10.8
W17386	321±28.9	293±27.8	42	192±5.22	160±6.37

Table 3. Single grains measured and acceptance data*

Sample	N	No signal	Too high	Other rejections	accepted	Acceptance rate (%)
UW3726	779	556	107	42	74	9.5
UW3727	873	636	105	43	89	10.2
UW3728	967	721	130	48	68	7.0
UW3729	970	703	162	27	78	8.0
UW3730	385	266	61	20	41	10.6
UW3731	294	185	63	12	34	11.6
Total	4268	3067	628	189	384	9.0

* Rejection criteria: "No signal" refers to grains that lacked a measurable signal, as judged by an error greater than 30% on the test dose or a natural signal that was not at least three standard deviations above background. "Too high" refers to grains where the natural signal was larger than the signal from the highest regeneration dose and thus did not intersect the growth curve. Other rejections include failed recycling where the ratio of the corrected signals from two identical regeneration doses did not fall within 0.8 and 1.2, recuperation where the signal from a zero dose was more than 10% of the natural signal and the decay curve showed a definite downward slope, feldspars deemed such because of loss of signal from an IRSL stimulation, and zero doses where the derived equivalent dose was not significantly different from zero.

Table 4. Single-grain D_e and age

Sample	CAM D_e (Gy)	Over-dispersion (%)	CAM age (ka)	Largest FMM D_e (Gy) *	Proportion (%) *	FMM age (ka)
UW3726	46.5±3.28	44.1±6.4	39.1±3.51	51.3±2.56	88.8	43.2±3.2
UW3727	35.8±2.85	60.5±6.7	18.2±1.88	76.6±5.17	23.0	39.0±3.7
UW3728	42.8±2.87	37.2±6.3	28.1±2.71	58.5±3.40	62.6	38.4±3.5
UW3729	46.8±3.12	40.4±6.3	33.3±3.07	53.8±2.96	87.9	38.2±3.2
UW3730	54.5±6.0	49.4±10.2	53.8±6.09	76.5±7.25	73.9	53.7±6.1
UW3731	75.8±6.43	28.6±9.1	50.5±5.72			

* FMM divides distribution into single-aged components given an over-dispersion considered typical of a single-aged sample (10% in this case). The value given is the average age of the component with the largest D_e. An exception to this is for UW3726 where the 2nd largest component is given, because the largest contains only 2.1% of the grains. The values under "proportion" are the proportion of grains assigned to the largest FMM component. For UW3731, the total distribution is consistent with the central age value, possibly because of small sample size.

Table 5. Characteristic doses and D_e values for UW3827

Characteristic dose (Gy)	# accepted	D_e (Gy)	# "too high"*
< 21.5	9	16.8±6.40	38
21.5 - 30	16	25.9±3.90	31
31 - 60	24	41.9±4.34	23
> 61	42	43.1±4.26	5

* Defined in Table 4.

Table 6. Acceptance rates for K-feldspars*

Sample	n	No signal	Too high	Other rejections	Accepted	No finite fading correction	Rate (%)
UW3726	293	190	11	27	65	6	22.2
UW3727	394	180	63	53	98	9	24.9
UW3728	193	44	32	36	81	6	42.0
UW3730	393	142	105	33	113	25	28.8
UW3731	387	174	66	64	83	17	21.4
Total	**1660**	**730**	**277**	**213**	**440**	**63**	**26.5**

* Rejection criteria: "No signal" refers to grains that lacked a measurable signal, as judged by an error greater than 30% on the test dose or a natural signal that was not at least three standard deviations above background. "Too high" refers to grains where the natural signal was larger than the signal from the highest regeneration dose and thus did not intersect the growth curve. Other rejections include failed recycling where the ratio of the corrected signals from two identical regeneration doses did not fall within 0.8 and 1.2, recuperation where the signal from a zero dose was more than 10% of the natural signal and the decay curve showed a definite downward slope, and zero doses where the derived equivalent dose was not significantly different from zero.

Table 7. Equivalent dose, fading and age data – K-feldspars

Sample	n	Equivalent dose (Gy)	Average g-value (%/decade)	Corrected age (ka) Central age model	Over-dispersion (%)	Corrected age (ka) Largest component (% of grains)
UW3726	65	78.0±10.1	4.16±0.80	62.6±11.5	111±14.6	116±8.56 (76%)
UW3727	98	103.9±7.19	3.95±1.01	62.9±5.65	58.8±7.5	83.6±6.30 (67%)
UW3728	81	98.5±7.12	2.77±0.64	80.3±6.35	52.6±6.6	63.8±6.98 (50%)
UW3730	113	88.2±4.58	9.02±1.47	68.7±4.92	36.9±6.8	71.2±3.43 (96%)
UW3731	82	73.9±5.17	7.73±2.31	55.7±4.72	42.8±7.3	70.0±4.18 (72%)

Table 8. post-IR $IRSL_{290}$ results.

Sample	N	No finite fading correction	Corrected age (ka)	Over-dispersion (%)	Uncorrected age (ka)	Over-dispersion (%)	Uncorrected Age (ka) – largest component (% of grains)
UW3726	36	4	46.4±9.36	103±15.4	44.0±8.06	108±13.7	103±7.93 (44%)
UW3727	38	0	59.1±10.8	90.5±14.1	50.8±7.52	86.1±11.0	79,1±4.97 (62%)
UW3728	55	0	105±9.54	49.1±7.8	89.1±6.76	48.0±6.2	136±12.7 (49%)
UW3730	13	7	68.9±15.0	41.6±22.2	69.3±6.20	29.0±8.2	89.2±9.93 (55%)
UW3731	11	1	86.2±15.2	44.2±15.5	68.6±12.0	55.8±13.4	101±8.82 (73%)

Table 9. Southern Africa MSA layers dated around 70-80ka and their industrial/archaeological attribution.

Name of the site	Layer	Chronology		Method	Industry	Publication/s
Bushman Rock Shelter	28	73±6 ka (quartz)	91±10 (feldspar)	OSL	Pietersburg	Porraz et al., (2018)
		75±6 (quartz)	97±10 feldspar)			
Blombos	CGAA CGAA CFD CFB/CFC CFB/CFC CFA CD CC CC CA BZB CAB CAC CCh1 CCh1	78.8 ± 5.6 78.9 ± 5.9 76.7 ± 4.8 68.8 ± 4.6 75.5 ± 5.0 69.7 ± 3.9 74.9 ± 4.3 72.5 ± 4.6 74.6 ± 3.9 73.3 ± 4.4 81 ± 10 66 ± 7 77 ± 8 64 ± 6 79 ± 8		OSL TL	Still Bay	Jacobs et al. (2003a,b)
Border Cave	4 BS 1 RGBS BC5 fossil 3 WA 3 BS3			ESR	Howiesons Poort	Grün et al. (2003)
Die Kelders	Layer 11 Layer 9 Layer 7	70.3 ± 5.8 79.7 ± 15.6 75.3 ± 6.8		OSL	MSA	Feathers and Bush (2000)
Diepkloof	Logan Kate/Keny	73.6 ± 2.5 70.9 ± 2.3		OSL	Still Bay/Howiesons Poort	Porraz et al., (2008) Tribolo et al.,

					(2013)
Hollow Rock		80.0 ± 5.0 72.0 ± 4.0	OSL	Still Bay	Högberg and Larsson (2011)
Klasies River, Cave 1/1A	SAS Member Layer 22 from (Singer and Wymer excavations	70.9 ± 5.1 72.1 ± 3.4	OSL	MSA II Pre-Howiesons Poort	Feathers (2002) Jacobs et al, 2008
Klasies River Cave 2	RF Member (Deacon ex.)	71.6 ± 2.9	OSL		Jacobs et al., (2008)
Melikane	Carter Layer 6	79.5 ± 3.1	OSL	MSA	Stewart et al. (2012)
Pinnacle Point 5–6	SADBS	70.6 ± 2.3	OSL	Microlithic MSA	Jacobs (2010)
Rose Cottage	KUA LEN LEN	71.4 ± 4.2 72.5 ± 6.8 76.3 ± 14.8	OSL	Pre-Howiesons Poort	Valladas et al., (2005)
Sibudu	RGS LBG LBG2 BS	70.5 ± 2.0 72.5 ± 2.0 73.2 ± 2.3 77.3 ± 2.2	OSL	Still Bay Pre-Still Bay	Jacobs et al., (2008)

Dear Editor,

All the authors declare no conflict of interest regarding this research.

Yours sincerely,

Paloma de la Peña

Johannesburg, 8th July 2019